Constructability-based design approach for steel structures: From truss beams to real-world inspired industrial buildings

Automation in Construction 166 (2024) 105630

Contents lists available at ScienceDirect

Automation in Construction

journal homepage: www.elsevier.com/locate/autcon

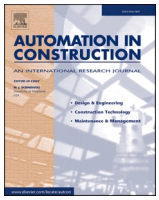

Constructability-based design approach for steel structures: From truss beams to real-world inspired industrial buildings

Raffaele Cucuzza [a,*], Angelo Aloisio [b], Majid Movahedi Rad [c], Marco Domaneschi [a]

[a] Department of Structural, Geotechnical and Building Engineering, Politecnico di Torino, Turin, Italy
[b] Department of Civil, Construction-Architectural and Environmental Engineering, Università degli Studi dell'Aquila, L'Aquila, Italy
[c] Department of Structural and Geotechnical Engineering, Széchenyi István University, Győr, Hungary

ARTICLE INFO

Keywords:
Steel structures
Constructability
Size optimization
Shape optimization
Topology optimization
Grouping strategy

ABSTRACT

This paper presents an optimization framework for steel trusses. The authors implemented a penalty-based approach to optimise the size, shape, and topology based on a dynamic grouping strategy to address the constructability challenges. The main contribution of the paper is the use of damped exponential constructability penalties. This approach ensures optimal designs by balancing structural complexity, through standardization in design, and minimizing the total number of members and variety of sections, with the overall structural cost. The paper also presents a detailed analysis that underscores the sensitivity of the optimization convergence to the algorithmic hyperparameters, emphasizing the role of cross-section assignments and stabilization of truss piece counts. The optimization framework is validated on a trussed roof structure based on the findings from the single truss optimization. The best truss topology proved to be the Howe truss configuration, highlighting its efficiency in meeting the defined objective function.

1. Introduction

Civil engineering design problems are inherently complex due to many decision variables and regulatory constraints. Optimization algorithms have emerged as highly effective tools for addressing these challenges, directly or indirectly. Indirect applications of metaheuristics involve their integration with other AI-based techniques, such as artificial neural networks [1–3], genetic programming [4], fuzzy logic [5,6], support vector machines [7], random forests [8], hybrid [9], and more. These combinations enhance their effectiveness in tackling complex civil engineering design problems. Optimization algorithms [10] and, specifically, population-based metaheuristic algorithms [11–17], have also demonstrated their importance in handling challenging civil engineering design problems without additional techniques [18–21].

A typical structural optimization problem in civil engineering involves steel trusses [22]. Typically, the optimization problems fall into three distinct categories: (i) size, (ii) shape, and (iii) topology optimization.

There is extensive literature on steel truss optimization, with leading research trends: (i) exploring novel optimization methods also dealing with uncertainty estimation and for solving high-dimensional or large-scale problems, (ii) considering advanced structural analyses, and (iii) improving the optimization problem formulation (multi-objective optimization, including new regulatory compliance, real-time design and digital twins, prefabrication and additive manufacturing, incorporating sustainability and environmental impact, e.g. [23,24]).

The first research path might be considered the most explored due to several factors, such as the increased computational power, the range of applications, the complex problem solving, the increasing trend towards data-driven decision making, interdisciplinary research and machine learning integration [25–28]. Specifically, high dimensional optimization of trusses [29] (i.e. high number of elements and design variables) represents a challenging scenario where researchers developed efficient optimization strategies guaranteeing convergence towards global solutions with limited computation effort [30–33]. Recently, new numerical experiments, as well as benchmark tests, have been developed to address this scope [34,35].

Moreover, regarding the first research path, the extensive literature is also oriented on applying novel optimization approaches, mainly population-based, to optimise steel structures [36–41].

Regarding the second research aspect, the optimal design of steel truss structures, with a focus on accurately approximating inelastic

* Corresponding author.
E-mail addresses: raffaele.cucuzza@polito.it (R. Cucuzza), angelo.aloisio1@univaq.it (A. Aloisio), majidmr@sze.hu (M.M. Rad), marco.domaneschi@polito.it (M. Domaneschi).

https://doi.org/10.1016/j.autcon.2024.105630
Received 22 January 2024; Received in revised form 10 July 2024; Accepted 10 July 2024
Available online 23 July 2024

structural responses such as load-carrying capacity, has gained significant attention [42–45]. The design of steel structures inherently involves the consideration of high-order nonlinear formulations that originate from the inelastic material properties, resulting in nonconvex feasible domains.

The third research path, related to problem formulation, is more connected to design and engineering practice. This paper falls within such third path to address constructability in the optimal design of steel trusses, taking size, shape, and topology design variables into consideration.

Constructability is a pivotal aspect of civil engineering structural design, significantly influencing the success of construction projects [46]. Broadly, it encompasses technical and practical considerations such as transportability, joint connections [47], and efficient utilization of materials and resources, all of which come into play during the realization phase—comprising production, assembly, and erection [48]. In 1986, the Constructability Task Force of the Construction Industry Institute (CII) at The University of Texas defined Constructability as "the optimal integration of construction knowledge and experience in planning, design, procurement, and field operations to attain overall project objectives." In the United Kingdom, "buildability" was introduced as a term defined as "the extent to which the design of the building facilitates ease of construction while meeting overall building requirements." Anderson et al. [49] defined it as "the capability of being constructed."

This study aims to integrate construction knowledge, resources, technology, and experience into the engineering and design of steel buildings [50–52]. As illustrated by several authors [53–55], the early design phase presents the best opportunity to impact project costs. Therefore, incorporating constructability during the initial design phases is crucial for cost control, e.g. [56].

One of the most adopted methods for addressing constructability is standardising structural components. In general, using standardized components and systems leads to an improvement in constructability by reducing the need for custom fabrication and assembly. The idea of standardization has been defined, by Pasquire et al. [57], as "the extensive use of components, methods or processes with regularity, repetition and a successful history". Wong et al. in [58,59], also explained how standardization can be translated as the repetition of grids, sizes of components and connection details, stressing the benefits in terms of faster construction, reduced number of mould changes and enhanced productivity.

In this sense, numerous scientists focused on reducing the high variety of profiles commonly suggested by optimized designs with optimal grouping strategy [60–64]. Recently, this aspect has been faced with clustering approaches via Neural network [65], fully stressed design [66,67], adding cardinality constraints [68] and, as adopted in the current paper, by directly adapting the objective function (OF) with proper penalty functions [69,70]. In summary, standardization comprehends different meanings, from the use of standard elements in the design of a structure [71] to avoiding particular and unique shapes or sections, the repetition of members [72] and connections [73].

This paper expands the preliminary results obtained in a previous work [74] and introduces an innovative optimization approach applicable to a broad spectrum of steel structures, ranging from truss beams to real-world industrial buildings. This approach, built upon a penalty-based optimization framework employing three distinct penalty functions (ϕ_1, ϕ_2, and ϕ_3), tackles the structural design while encouraging the standardization of steel members (i.e. the number of different sections and the total number of employed pieces) and reduction of constructability issues along the construction process. Specifically, the method assigns cross-sections based on stress distributions within truss beam optimization. It optimizes size, shape and topology, employing a dynamic grouping strategy that effectively reduces overall weight while preserving the structural feasibility of the engineering solutions (e.g. realistic design) and robustness [75–78]. The scope of this investigation extends to the domain of industrial building design, revealing how the optimization of truss beams dynamically influences the larger-scale structure.

The novelty of this research compared to existing literature lies in its comprehensive approach to steel structure optimization achieved by an innovative problem statement of the optimization process where penalty functions have been calibrated for assuring competitive structural performance by limiting troubles during the assembly phase and reducing potential cost during the production phase of steel pieces. While prior studies have predominantly focused on specific aspects of structural optimization mainly related to computational efficiencies of the algorithms, this paper integrates these facets into a unified framework in which dynamic grouping strategy and constructability aspects are considered to ensure ease during the operational procedures in situ and a significant reduction of the overall structural complexity. This strategy significantly reduces final weight while ensuring structural integrity, offering an innovative solution to a long-standing optimization challenge.

The research paper is organized into three main parts: the problem formulation and the analysis of two case studies, a planar truss and a real steel industrial building.

2. Problem formulation

This section introduces the problem formulation, beginning with the mathematical background and then moving on to its practical implementation using commercial software tools: Grasshopper, Karamba3D, and Octopus.

2.1. Mathematical background

The primary objective of this paper is to achieve an optimal design that considers structural constraints and constructability issues to streamline construction complexity.

The objective function can be computed as follows:

$$min: f = \rho \sum_{i=1}^{N} (A_i \cdot l_i) \cdot \phi_1 \cdot \phi_2 \cdot \phi_3 \tag{1}$$

with design variables defined in the domain

$$x_{min} \leq x \leq x_{max} \tag{2}$$

Where N is the total number of elements in the truss, with different values based on the truss typology selected by the optimizer at each iteration; ρ is the mass density of structural steel $S235$ (EN10025–2, European Code), equal to 7850 kg/m^3, A_i is the area of the i-th member, l_i is the length of the i-th member. Vector $\boldsymbol{x}$ collects the problem's generic design variable (DV) of the problem, categorized into three different optimisation levels (Size, shape, and topology). According to the specific case study, the DV's vector will be expanded with a detailed description of each component and their influence in the OF will be described.

The penalty functions are ϕ_1 and ϕ_j defined as:

$$\phi_1 = \begin{cases} 1 \text{ if } n_{un} = 0 \\ (1 + K_1 \cdot n_{un}) \text{ if } n_{un} \geq 1 \end{cases} \tag{3}$$

where K_1 is a proportional constant and n_{un} the number of unfeasible individuals. Specifically, ϕ_1 is the penalty function associated with the structural safety of the structure. Eq. 3 displays a linear relationship that is directly proportional to the number of unfeasible individuals (n_{un}) at each iteration. In this way, not only the level of violation but also the cardinality of the unfeasible elements has been considered.

The number of unfeasible elements n_{un} is estimated by evaluating the following design inequalities based on European regulation. Specifically, Eq.s 4 and 5, concerning the combined bending and axial force as well as buckling verification under flexure and axial compression, has been implemented according to EC3 6.3.3. [79], respectively. These

verifications have been conducted with specific regard to columns and roof beams (i.e. purlins) within case study No.2:

$$\frac{N_{Ed}}{N_{Rd}} + \sqrt{\left(\frac{M_y^{Ed}}{M_y^{Rd}}\right)^2 + \left(\frac{M_z^{Ed}}{M_z^{Rd}}\right)^2} < 1 \tag{4}$$

$$\frac{N_{Ed}}{\chi_a \cdot N_{Rd}} + \sqrt{\left(k_{ay} \cdot \frac{M_y^{Ed} + N_{Ed}.e_{N_y}}{\chi_{LT} \cdot M_y^{Rd}}\right)^2 + \left(k_{az} \cdot \frac{M_z^{Ed} + N_{Ed}.e_{N_z}}{M_z^{Rd}}\right)^2} < 1 \tag{5}$$

while, for truss elements only (i.e. case study No.1), structural checks under pure compression and tension axial forces have been implemented according to EC3 6.3.3. [79]:

$$\frac{N_{Ed}}{N_{t,Rd}} \leq 1 \tag{6}$$

$$\frac{N_{Ed}}{N_{c,Rd}} \leq 1 \tag{7}$$

$$\frac{N_{Ed}}{N_{b,Rd}} \leq 1 \tag{8}$$

$$u_{y,max} \leq u_{y,lim} \tag{9}$$

where N_{Ed} is the design axial force, $N_{t,Rd}$, $N_{c,Rd}$ and $N_{b,Rd}$ are the tensile, compression and buckling capacity of the generic truss element, respectively. Accordingly to the type of section (i.e. Circular hollow section) and grade of steel, class of section equal to 3 and buckling curve c have been adopted coherently with EC3 6.3.1.2 Table 6.2 [79]. In eq. 9, $u_{y,max}$ is the design deflection of the truss, while $u_{y,lim}$ is the limit deflection value. The latter, in the case of steel civil building, is assumed to be equal to $L/200$, with L being the total span of the truss beam coherently to the suggestion provided by Italian standard regulation.

The remaining penalty function ϕ_j is defined as

$$\phi_j = (1 + a_j) - e^{-b_j \cdot \left(P_j - \frac{\ln a_j}{b_j}\right)} \tag{10}$$

where a_j, and b_j are constants while P_j represents the *constructability* index and it is devoted to simulating the structural complexity during the construction process.

In this work, P_j is expressed by two distinct parameters as N_a and n which represent the number of different cross-sections and the number of subdivisions in the truss, respectively. Hence, the ϕ_j penalty can be particularized as two distinct penalties ϕ_{N_a} and ϕ_n.

In contrast to penalty ϕ_1, ϕ_j (or ϕ_{N_a} and ϕ_n penalties if explicitly declared) takes on an exponential form with a damping effect governed by negative exponential coefficients [80,81]. Eq. 3 guides the algorithm to assign feasible sections for each class of elements that satisfy the structural verification and serviceability conditions outlined in Eqs. 6–8 and Eq. 9, respectively. On the other hand, Eq. 10 primarily aims to reduce the overall construction complexity by managing the number of different sections, N_a, and the total number of pieces, n, employed for the truss layout definition.

Aiming to explore the benefits of adopting such a complex mathematical form expressed by Eq. 10, Fig. 1 has been reported. In this plot, a comparison between the standard linear penalty, ϕ^{linear}, and the damped exponential one, $\phi^{exp.}$, adopted by the authors, has been represented. With specific regard to the latter, three different levels of penalization have been depicted by varying the b_j parameter: high, medium and low penalty levels. If ϕ^{linear} guarantees a proportional level of penalty when the number of employed sections increases, $\phi^{exp.}$ reduces the "goodness" of the solution as the *structural complexity* index, p_j, increases. In other words, how the penalty increases, represents a substantial difference

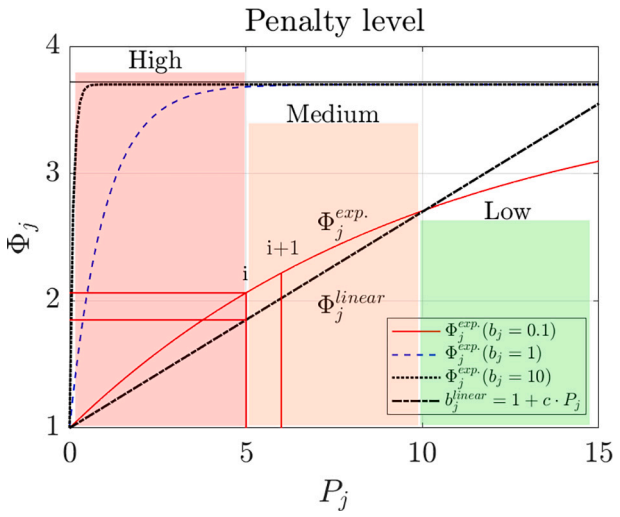

Fig. 1. Comparison between standard linear penalty and the damped exponential one adopted by the authors.

between the two penalty approaches. In this sense, the slope of the curve represents a "decreasing speed" of the complexity cost which tends to an asymptotic value. While by adopting the constant penalty the increase between step i and step $i+1$ is always the same, in the exponential penalty, it varies according to the b_j value.

In conclusion, following the latter approach, the optimizer is guided to appreciate better the variation of weight as a compromise between the increase of mass and the increase of the structural complexity. Even if, as in the graphical example shown in Fig. 1, the linear penalty could assume values lower than the exponential one, it leads to optimal designs characterized by low structural complexity (i.e. few employed sections or total number of pieces) but with an unsustainable increase of the total cost (i.e. weight) of the structure.

2.2. Design variables

The design variables are grouped after the optimization goals, size, shape and topology. After establishing the general truss layout selected by the optimizer randomly, the structure's sizing was determined by allocating predefined sections to each group of elements following the evolutionary criteria of SPEA-II. These sections were selected from a European standard list based on Eurocode 3, containing almost 100 feasible Circular Hollow Sections (CHS) profiles. This choice aligns with practical recommendations and facilitates assembly. The main shape and topology variables are represented in Fig. 2 and the lower and upper bounds are collected in Table 1 where practical recommendations derived from the experience have been adopted.

The shape optimization variables include the number of subdivisions of half the chords (n), as well as the heights at the edges (H_1) and the midpoint (H_2) of the upper chord. To define the permissible range for n it was constrained to values between 3 and 10. The upper bound was

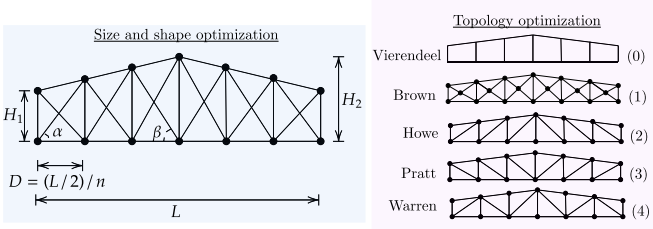

Fig. 2. Illustration of the size shape and topology optimization by expressing the design variables.

Table 1
Main design variables considered for the truss optimization.

Design variable	Minimum	Maximum
H_1	max $[L/15, Dtan(30^o)]$	min $[H_1, Dtan(60^o)]$
H_2	max$[L/10, Dtan(30^o)]$	min $[L/8, Dtan(60^o)]$
n	3	10
n_t	(0) Vierendeel, (1) Brown, (2) Pratt, (3) Howe, (4) Warren.	

determined with a minimum distance of 1 m between consecutive nodes. The span length of the truss was assumed to be equal to 20 m. The selection of the boundaries in Table 1 follows [82].

Topology optimization involves the selection of five truss typologies through the discrete variable $n_t \in \{0, 1, 2, 3, 4\}$: (0) Vierendeel, (1) Brown, (2) Pratt, (3) Howe, and (4) Warren, as depicted in Fig. 2. These truss types are chosen based on their suitability for various engineering challenges and applications, making them valuable options in structural design.

The Vierendeel truss is characterized by the absence of diagonal members and vertical struts in tension. As distinct from the other truss typologies, it must be realized with fully-restrained joints for preserving instability when horizontal actions only are considered. It is commonly employed in civil engineering structures, offering an aesthetically pleasing configuration. With its X-shaped diagonals, the Brown Truss ensures that one member of each X-component is always in tension. It is preferred for applications where actions may invert during the structure's service life, such as wind loads or seismic actions, even though it results in heavier designs. The Howe truss, with symmetrical compressed diagonals relative to the axis of symmetry, excels in situations where uplift actions are predominant, such as open buildings like aircraft hangars or factories. The Pratt truss, renowned for achieving long spans typically ranging from 20 to 100 m, features compressed and tensioned diagonal members, making it suitable for handling predominantly horizontal actions. The Warren truss, known for its versatility, features an upper chord in compression and a lower chord in tension. Diagonals switch from tension to compression at the midpoint. Alternate vertical elements help distribute compression forces for long spans. This truss type finds widespread use in civil engineering, especially for steel railway bridges.

2.3. Grouping strategy

A two-level grouping strategy has been devised to highlight the engineering solutions achieved through the optimization process, starting from the preliminary design phase. The fundamental concept is to gather elements with similar mechanical properties, such as compression or tension and stress levels, as illustrated in Fig. 3. This approach guides the algorithm towards minimizing structural complexity and overall cost. Employing different sections for every member in practical structural design is often impractical. Additionally, the assembly and erection processes favour installing entire truss sections at once. Consequently, organizing elements into groups with shared mechanical characteristics results in more feasible engineering solutions.

As evidenced by several authors [75–78], the grouping strategy's effectiveness is closely linked to the structure's level of symmetry. In this study, leveraging the symmetry around the vertical axis, an initial grouping stage has been conducted, resulting in the classification of five distinct truss components: (i) Upper Chord and External Vertical Struts; (ii) Lower Chord; (iii) Internal Vertical Struts; (iv) Upward-Downward Diagonals; (v) Downward-Upward Diagonals, as shown in Fig. 3.

After obtaining the initial grouping of elements, a second-level classification has been established, considering the actual stress levels within each group of elements. To illustrate this second-level grouping strategy, a visual representation in Fig. 4 has been adopted, focusing on the lower chord (the same applies for the other truss components). Within each selected truss component, every member has been categorized into one of three primary classes based on the stress level experienced by the structure. Fig. 4 offers insight into the stress distribution along the lower chord, highlighting three distinct inflexion points in the axial tension force diagram and explaining the rationale behind each group's identification.

The optimiser is configured to dynamically categorise elements into different sections to promote optimal design with cost savings and discourage overly complex structural solutions. This categorization changes at each iteration based on the specific transition point identified. In Fig. 4, three distinct groups are considered, with two cutting indices positioned at nodes 3 and 5. More in detail, when dividing the lower chord into three groups, two indexes need to be identified, I_1 and I_2. To avoid overlapping between groups of sections, n_1 may assume a value ranging between 1 and $n - 2 = 4$, while n_2 in between $n_1 + 1$ and $n - 1 = 5$ where n represents the number of subdivisions of the lower chord. Following this scheme, the optimiser could investigate all the possible numbers of section groups until $N_{groups} = N_{subdivisions} \cdot n$.

2.4. Implementation

The software implementation of the proposed methodology includes the interaction among (i) Rhinoceros [83], (ii) grasshopper [84], (iii) Karamba [85] and (iv) Octopus [86].

Data from the geometric Rhinoceros model is transferred from the Grasshopper parametric model to the Karamba FEM solver. Subsequently, the solver feeds the analysis results into the Octopus optimizer. Initially, the elements created as basic geometry in Grasshopper are transformed into FEM components. This transformation involves specifying cross-sections, materials, joints, supports, and applied loads. The "Utilization of elements" component is then used to examine the structural verification results, adhering to the guidelines of EN 1993-1-1 within Eurocode 3 [79].

The optimization process relies on the well-established Strength Pareto Evolutionary Algorithm (SPEA), initially proposed by Zitzler [87–89]. An enhanced iteration of this algorithm, known as SPEA-II and also introduced by Zitzler [90], is integrated into the Octopus plugin. This algorithm's effectiveness has been rigorously demonstrated across various multi-objective design domains, as shown in [91,92]. In this study, this metaheuristic technique has been adopted for solving single-objective optimization problems [93]. Aiming to demonstrate the feasibility of the proposed approach, SPEA-II has been tested on classic numerical benchmarks and compared with other well-known algorithms which are acknowledged to work well with discrete design of 2D and 3D trusses. Its reliability in terms of convergence capability and robustness has been demonstrated on a similar class of problems by validating the results obtained in this work. All the details and the results of the analysis have been reported in Appendix A.

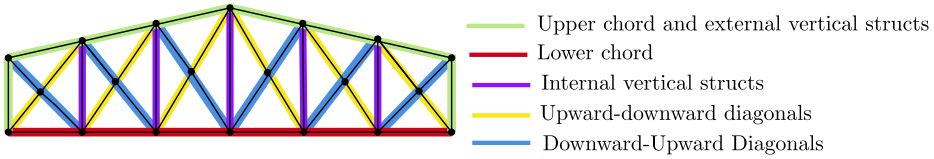

Fig. 3. First-level grouping strategy of a Brown truss. (For interpretation of the references to colour in this figure legend, the reader is referred to the web version of this article.)

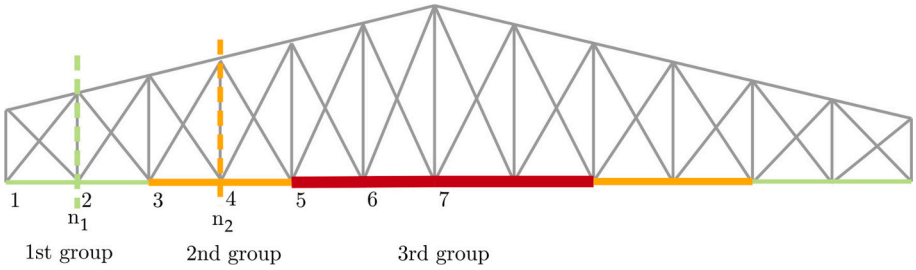

Fig. 4. Second-level grouping strategy of the lower chord of a Brown truss based on the stress level. (For interpretation of the references to colour in this figure legend, the reader is referred to the web version of this article.)

Table 2 outlines the key parameters and settings used in the optimization algorithm. It is worth noting that some of the parameters set differ between case studies No.1 and No.2. Due to the different computational efforts required and the total number of DVs involved by the two case studies, the authors decided to increase the level of exploration and exploitation by fixing higher value of maximum iterations and population size for the optimization process of the real-world inspired industrial building (Case No.2).

For case studies No.1 and No.2, the algorithm is allowed to run for a maximum of 250 iterations, respectively, to search for optimal solutions effectively. A population of 200 and 400 potential solutions is maintained in each iteration to explore various design possibilities for each case study. The crossover probability is performed with a 70% probability in each iteration, allowing for the exchange of genetic material between potential solutions. Additionally, the Elitism operator has been selected and the percentage of new solutions that are bred out from the entire pool has been fixed; if high, more local optimization is performed. In this case study, this percentage was set to 20% in order to make sure that the best individuals are not discarded, by transferring them directly into the next generation. Moreover, it was set that the 2% of the best unfeasible individuals survived to the next generation in order to guarantee diversity inside the new population. The mutation probability (0.05) controls the likelihood of introducing small random changes in potential solutions, promoting diversity within the population. The convergence threshold for the OF is set to 0.001. Basic Tournament selection is employed to choose potential solutions for reproduction, ensuring that fitter solutions are more likely to be selected [94,95].

Figure 5 overviews the flowchart showing the main steps of the optimization process. Once the structural geometry has been parametrically modelled in Grasshopper, each element comprising the structure is transformed into Finite Element Method (FEM) elements by utilizing Karamba3D components. These elements are equipped with assigned cross-sections, loads, and supports.

3. Case no.1: 2D steel truss

The first case study is a planar truss with a span length of 20 m. The 2D modelling of each truss typology has been conducted aiming to reproduce the only axial (e.g. tension/compression) behaviour of bars except the Vierendeel truss for which fully-restrained joints have been considered. Simply-supported static scheme has been assumed for each truss system.

Table 2
Optimization algorithm parameters and settings.

Parameter	Value
Maximum Iterations (Case No.1/No.2)	250
Population Size (Case No.1/No.2)	200/400
Mutation Probability	0.05
Crossover Probability	0.7
Convergence Threshold	0.001
Selection Mechanism	Tournament Selection
Penalty Functions	ϕ_1, ϕ_{N_a}, ϕ_n
Optimization Approach	Penalty-Based
Algorithm Integration	SPEA-II (Octopus Plugin)
Dynamic Grouping	Yes

3.1. Load definition and design variables

The gravitational loads are modelled following the Ultimate Limit State (ULS) combinations specified by the European Standard Regulation (EN 1993-1-1):

$$\gamma_{G1}\cdot G_1+\gamma_{G2}\cdot G_2+\gamma_P\cdot P+\gamma_{Q1}\cdot Q_{k1}+\gamma_{Q2}\cdot\psi_0 2\cdot Q_{k2}+\ldots \tag{11}$$

Here, G_1, G_2, and Q_{ki} represent the permanent structural loads, permanent non-structural loads, and variable loads, respectively. The coefficients γ are the partial safety factors determined based on the type of loads involved. The authors opted for the most critical scenario. In alignment with the practical application of this structure, an aluminium corrugated sheet was employed for the roof covering. All these forces were applied as concentrated loads at the upper nodes of each truss under investigation.

The calculated load values, along with their respective amplification factors, are summarized in Table 3:

Table 4 defined all the DVs involved in the optimization process, with their lower and upper bounds, and each category is colour-coded to assess its contribution to the final optimal design. Additionally, a graphical representation in Fig. 6 assigns each DV to specific groups of elements. For simplicity, the authors adopted a Brown truss typology as the model type, with three different cross-section groups (i.e., three cutting indices) adopted for each structure component, allowing the same variable to be assigned to elements belonging to the same group.

3.2. Penalty functions

In an optimization process based on a penalty approach, the definition and calibration of penalty functions play a crucial role in achieving successful and feasible solutions.

Following the mathematical definition of the *constructability* penalty ϕ_j, expressed by Eq. 10, it can be particularized as follows:

$$\phi_{N_a}=(1+a_1)-e^{-b_1\cdot\left(P_{N_a}-\frac{\ln a_1}{b_1}\right)} \tag{12}$$

$$\phi_n=(1+a_2)-e^{-b_2\cdot\left(P_n-\frac{\ln a_2}{b_2}\right)} \tag{13}$$

where a_1 and b_1 as well as a_2 and b_2 are the parameters that govern the final shape of the penalty functions ϕ_{N_a} and ϕ_n coherently with the final constructability target represented by the number of different sections, N_a, and the total number of pieces, n, respectively.

Especially for these penalties, It is worth noting that their geometric nature significantly affects the optimal design. In other words, the parameters tuning is not only vital to ensure convergence but it guides also the algorithm towards preferring solutions with a higher or lower

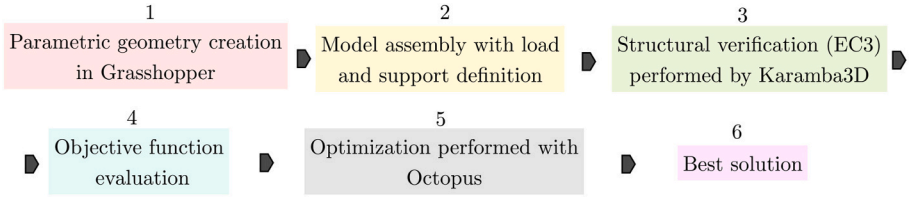

Fig. 5. Workflow of the algorithm implementation.

Table 3
Vertical loads applied to the truss structure.

Type of Load	Load Value	Coefficient γ
G_1	Self-weight	1.3
G_2 [kN/m^2]	1.471	1.5
Q_1 [kN/m^2]	0.5	1.5

Table 4
Design variables where the colors of the cells represent the different categories: blue - Topology; red - Layout definition; green - Grouping division; yellow - Cross-sections assignment.

Design variable	Description	Domain
x_1	Topology: (0) Vierendeel, (1) Brown, (2) Pratt, (3) Howe, (4) Warren	$0 \div 4$
$x_2 = n$	Number of subdivisions of half geometry	$3 \div 10$
$x_3 = H_1$	Heights of upper chord's edges	$H_{1,min} = max(\frac{L}{15}, D \cdot tan30)$ $H_{1,max} = min(\frac{L}{10}, D \cdot tan60)$
$x_4 = H_2$	Heights of upper chord's midpoint	$H_{2,min} = max(H_1, D \cdot tan30)$ $H_{2,max} = min(\frac{L}{8}, D \cdot tan60)$
$x_5 = n_1$	Index at which the third group ends	$1 \div n-2$
$x_6 = n_2$	Index at which the second group ends	$n_1+1 \div n-1$
x_7 x_8 x_9	3 sections for the lower chord elements	$0 \div 100$ CHS profiles' index from catalogue
x_{10} x_{11} x_{12}	3 sections for the upper chord + external vertical structs	$0 \div 100$ CHS profiles' index from catalogue
x_{13} x_{14} x_{15}	3 sections for the vertical internal structs	$0 \div 100$ CHS profiles' index from catalogue
x_{16} x_{17} x_{18}	3 sections for the upward-downward diagonals	$0 \div 100$ CHS profiles' index from catalogue
x_{19} x_{20} x_{21}	3 sections for the downward-upward diagonals	$0 \div 100$ CHS profiles' index from catalogue

number of pieces and/or different sections, respectively [81]. In this way, the parameters' tuning of penalties does not affect the searching ability of the algorithm. On the other hand, it represents a crucial step to assess the proper level of penalization achieving the preferable solution as a balance between total weight and structural complexity. This balance can be achieved according to the sensibility of the designer or the practical needs in the yard.

The parametric nature of this curve represents one of the novelties of this paper. Depending on the final aim of the designer or based on cost evaluations derived from production processes' considerations (e.g. concerning the production of steel pieces in the factory), the penalties change accordingly to the proper calibration of parameters a_1 and b_1, or a_2 and b_2.

The optimal values of these parameters, as presented in Table 5, were determined through a preliminary calibration procedure and suitable parameters tuning aiming to strongly penalize solutions with a total number of pieces and number of different pieces over 20 and 5, respectively. It was an arbitrary choice based on the specific class of problem and the final scope to encourage standardization by reducing constructability issues.

Specifically, in the case of K_1, the authors conducted size optimization for a Brown truss with $n = 6$ elements. No significant variation in the results has been observed, indicating that opting for an excessively high value of K_1 was unnecessary. Consequently, $K_1 = 10$ has been selected, as shown in Fig. 7(a).

For the penalty function ϕ_{N_a}, a_1 defines the asymptote beyond which further penalization has limited impact, while b_1 influences the curve's steepness before reaching the asymptote. The calibration of a_1 and b_1 began with the latter to establish the desired trend. Subsequently, by fixing the chosen b_1 value and specifying a particular N_a value to achieve the desired penalty level, a_1 was uniquely determined. The same approach has been performed for the other penalty ϕ_n.

As anticipated, when optimizing for minimum weight using only the penalty function ϕ_{N_a}, the solution with the fewest cross-sections for a Brown truss was obtained with $b_1 = 0.1$. As expected, a heavier final design, with respect to the traditional minimum weight approach, is the real cost to reduce constructability issues. In other words, reducing the structural complexity in terms of different cross-sections leads to an increase in the total weight of the structure. In this case, in fact, the optimizer is gradually guided along the assignment phase of the sections according to the soft stiffness of the curve obtained for the selected b_1 value. Furthermore, at higher values of b_1, the optimizer consistently selected the same number of different cross-sections, regardless of the level of penalization, as it struggled to discern variations in the penalty. In comparison to the prior scenario, there is a notable rise in the degree of penalization starting from the initial N_a values, aligning with the conspicuous steepness observed in the b_1 curve illustrated in Fig. 7. A similar trend emerged when employing a higher level of penalty.

In summary, lower values of b_1 shifted the asymptote towards higher values, resulting in a higher a_1. Lower b_1 values also led to a more gradual curve, resulting in more noticeable variations in the penalty function as the asymptote was approached. Considering all these factors, the authors determined that adopting $b_1 = 0.1$ represented the optimal trade-off aiming to find optimal designs with low structural complexity while preserving the slenderness of the structure.

Regarding the final penalty function, ϕ_n, complexity reduction was achieved by considering the number of truss subdivisions. An increase in n resulted in a higher total number of elements, more connections between the truss components, and increased overall cost. a_2 and b_2 played roles in setting the curve similar to a_1 and b_1, respectively. The authors used the same calibration procedure and set $b_2 = 0.1$. All values are summarized in Table 5.

This approach's main feature is its parameter flexibility for governing the penalty functions. This adaptability is an innovative facet of the proposed methodology. Designers can customize these curves to suit the building type or core design objectives, steering the final design towards their preferred solution.

The calibration procedure of these parameters has been conducted by following the graphical scheme reported in Fig. 8.

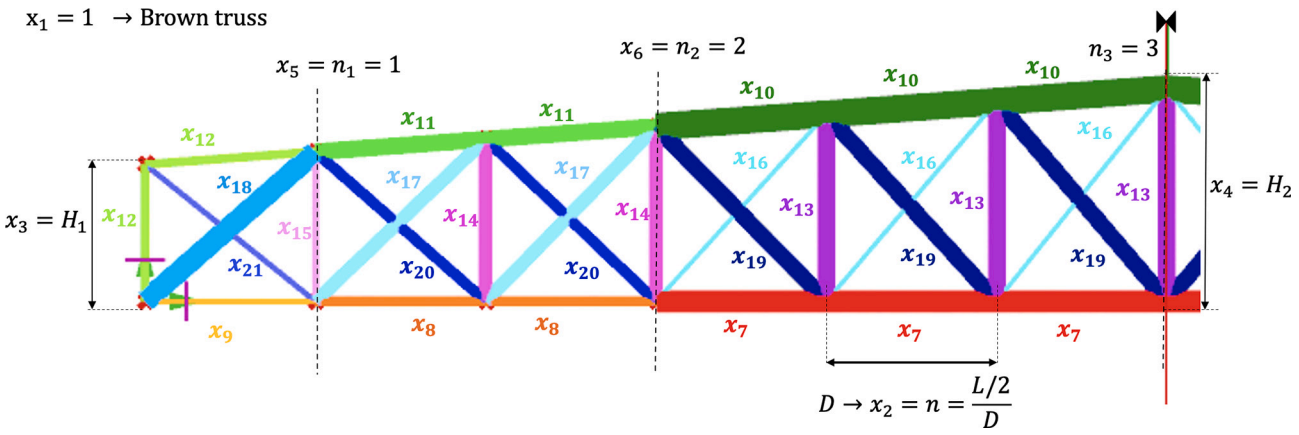

Fig. 6. Schematic representation of all the design variables.

Table 5
Penalties parameters.

Parameter	Value
K_1	10
a_1	2.70
b_1	0.1
a_2	1.157
b_2	0.1

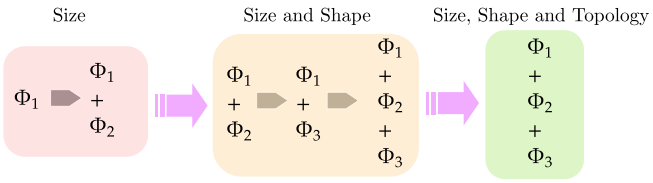

Fig. 8. Flow chart of the adopted penalties calibration.

3.3. Results

This subsection will show the results obtained by performing a simultaneous size, shape and topology optimization with all the different penalties ϕ_1, ϕ_2 and ϕ_3. The authors decided to focus mainly on discussing the results derived from the most representative case study in which the number of DVs (see Table 4) and the penalty approach contribute to fulfilling the final goal of this research. The sizing and the overall geometric layout are dynamically changed when the truss typology is selected parametrically. It should be remarked that topological optimization does not imply complete freedom in organizing the structural topology by varying the number, inclination, and connectivity at will [96–98]. On the contrary, due to the emphasized need to adhere to constructability criteria, the authors have identified five truss configurations: Vierendeel, Brown, Pratt, Howe, and Warren. Through a discrete variable x_1 (Table 4), the topological optimization is confined to selecting the best option from the aforementioned five typologies. To check the robustness of the optimization procedure conducted by the optimizer *Octopus* and the feasibility of the entire penalty procedure, 20 runs have been performed, and the results have been reported in Table 6.

All the obtained solutions have been arranged from the lowest to the highest OF. However, the lowest OF does not necessarily represent the

Table 6
Results of the best individual of each optimization for Size, Shape & Topology optimization.

No. run	Best OF	Weight [kN]	N_a	n	H_1	H_2	n_1	n_2	n_3	Topology
1	12.429	4.362	5	4	1.7	2.38	1	1	2	Pratt
2	12.435	4.143	5	5	1.53	1.96	1	1	3	Pratt
3	12.598	4.379	4	6	1.33	1.79	1	1	4	Pratt
4	12.604	4.424	5	4	1.97	2.39	1	1	2	Pratt
5	12.728	4.467	5	4	1.33	1.92	1	1	2	Pratt
6	12.776	4.644	4	5	1.55	1.85	1	1	3	Howe
7	12.853	4.282	5	5	1.38	2.17	1	1	3	Pratt
8	12.876	4.202	6	4	1.57	2.24	1	1	2	Pratt
9	12.881	4.683	4	5	1.59	1.85	1	1	3	Howe
10	13.069	4.587	5	4	1.33	1.86	1	1	2	Pratt
11	13.081	4.358	5	5	1.42	1.94	1	1	3	Pratt
12	13.144	4.613	5	4	1.34	2.06	1	1	2	Warren
13	13.173	4.623	5	4	1.38	1.95	1	1	2	Pratt
14	13.182	4.392	5	5	1.37	1.85	1	1	3	Pratt
15	13.317	4.125	6	5	1.56	2.05	2	1	3	Pratt
16	13.389	4.699	5	4	1.46	1.68	1	1	2	Pratt
17	13.480	4.731	5	4	1.76	2.48	1	1	2	Pratt
18	13.777	4.590	5	5	1.33	1.84	1	1	3	Howe
19	14.565	4.512	6	5	1.35	2.15	1	1	3	Howe
20	14.765	4.512	5	5	1.35	2.5	1	1	2	Howe

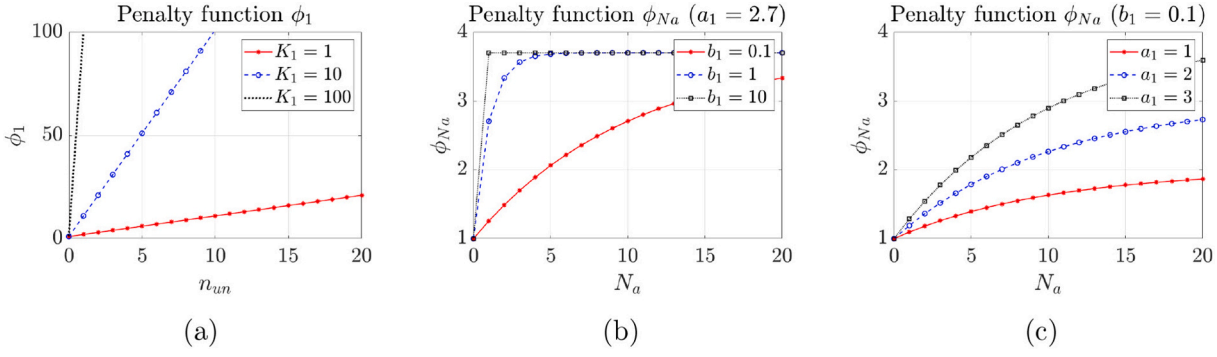

Fig. 7. Penalty function ϕ_1 changing k_1 and (b)-(c) penalty function ϕ_2 changing β and Δ.

lightest solution due to the nature of the penalty functions ϕ_2 and ϕ_3.

From this comprehensive overview, several preliminary observations can be made to identify potential trends among the optimal solutions: Initially, in most cases, the optimizer favours the Pratt configuration as the most promising solution in terms of cost-effectiveness across the entire solution set. The lowest weight, equal to 4.143 kN, was achieved for a Pratt truss with five different sections (N_a) and 5 number of subdivisions (n). Generally, the values of these two design variables range from 4 to 6, independent of the optimal truss typology identified by the optimizer. The best solution was obtained for values of H_1 and H_2 equal to 1.53 and 1.96, respectively. It's worth noting that the most promising solutions generally featured moderate values of H_2. Reducing this variable increased stress on the steel elements, but reducing bar length contributed to an overall weight reduction. Although all the solutions share the same number of cutting indices (i.e., n_1, n_2, and n_3), the effectiveness of the grouping strategy is demonstrated by the substantial variability in the number of elements belonging to the third group (n_3). This variability results from the differences in the number of employed sections, N_a, and the total number of pieces, n.

In conclusion, the primary challenge lies in the high dispersion of results. The large number of design variables, combined with the complexity of the OF resulting from numerous combinations of structural parameters, leads to significant result dispersion. However, despite the dispersion in OFs, the differences in corresponding structural weights can be considered negligible. Specifically, when comparing the total weight corresponding to the best OF with the average weight across all OFs, the difference is only 0.023 tons. Statistical features obtained by all the runs are reported in Table 7.

The cross-section assignment illustrates the algorithm's efficiency in identifying the optimal grouping strategy based on the applied stress levels. Fig. 9 showcases the optimal sizing of the best solution (Pratt truss). At the same time, the specific Circular Hollow Section (CHS) profiles assigned to each component are detailed in Table 8.

As also noted in [75], larger sections have been allocated from the edges to the middle span of the truss, aligning with the increasing stress levels along the tensioned bottom chord and the compressed upper one. Conversely, the opposite trend can be observed for the diagonals and vertical struts, where larger sections have been assigned to all Group 2 and Group 3 members.

The advantageous impact of the grouping strategy is evident from the fact that the same cross-section has been assigned to different elements belonging to various truss components (e.g., identical sections for the most stressed elements of the bottom chord, vertical struts, or diagonals). Consequently, a significant reduction in the number of different cross-sections is observed.

For clarity purposes, the trend of the most representative structural parameters of the best solution is depicted in Fig. 10. Specifically, due to the nature of the penalties ϕ_2 and ϕ_3, OF including penalties contribution and the only weight have been depicted for clarity purposes. Additionally, information about the unfeasibility proportion for each iteration (i.e. ratio between the number of unfeasible individuals and population size) has been reported to show the promising level of exploration of the algorithm.

Finally, a summary of all the results obtained by performing several optimization processes with different levels of penalties and groups of DVs has been reported in Table 9 as result of the calibration procedure described in the previous section.

Table 9 demonstrates that the inclusion of penalty functions (ϕ_2 and ϕ_3) in addition to ϕ_1 leads to higher structural weights. This is expected since the penalty functions penalize deviations from constraints, making achieving the same structural efficiency as in the ϕ_1-only cases challenging. It emphasizes the importance of selecting appropriate penalty functions based on the optimization objectives. Parameters that are kept fixed (highlighted in red) significantly influence the optimization outcomes. For example, fixing the number of subdivisions (n) and heights (H_1 and H_2) leads to consistent values across cases with the same fixed parameters. This suggests that these parameters play a determinant role in the optimization process. Regarding the grouping Strategy, the values of n_1, n_2, and n_3 in the grouping strategy impact the number of different cross-sections (N_a) used in the truss. More cutting indices (n_1, n_2, and n_3) generally lead to more sections, affecting the structural weight.

Table 7
Best, Worst, Mean and Standard deviation values of the OF for the considered Size, Shape & Topology optimization.

Best	Worst	Mean	Standard Deviation
12.429	14.565	13.072	0.509

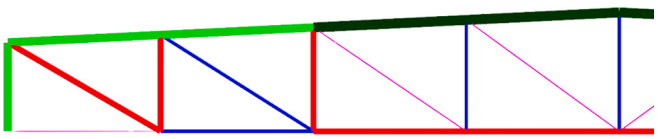

Fig. 9. Configuration of the optimized truss, obtained from the considered size shape and topology optimization.

Table 8
Cross-sections of the optimized truss.

Structural element	CHS First group	CHS Second group	CHS Third group
Lower Chord	101.6 × 2	60.3 × 2	21.3 × 2
Upper Chord + Ext. Vert. Structs	168.3 × 3	139.7 × 3	139.7 × 3
Int. Vert. Structs	60.3 × 2	101.6 × 2	101.6 × 2
Downward-Upward Diagonals	21.3 × 2	60.3 × 2	101.6 × 2

4. Case no.2: 3D steel structure

A real-world case study has been considered to validate the proposed approach, encompassing all the constructability aspects discussed in previous sections.

The building under investigation is located in the industrial area of "Mirafiori" in the South-West zone of Turin, Italy. The building represents a disused area that once housed activities of the famous FIAT company which was built in the early 60's. It was built entirely by steel trussed frames supported by steel coupled sections and a roof realized by corrugated sheets. In Fig. 11-(a), a picture of the inner spaces of the building is reported where the static scheme of the trussed frames can be appreciated.

As in the previous case study, the optimization aims to minimize structural complexity. This complexity is gauged by considering the total number of components utilized in construction and the diversity of cross-sectional profiles employed.

4.1. Parametric modelling and load definition

Much like the previous study on truss beams, this investigation involves the creation of a parametric building model. This is achieved by replicating predefined modules at a specified span distance, referred to as variable s in the optimization problem.

The 3D modelling of the structure has been realized by following the same strategy described in section 3 for trusses supporting the roof while *beam* elements have been used for columns and purlins. Elastic hinges have been adopted to connect trusses to columns as a common solution for this type of structure. Roof and vertical bracings have been modelled as *tension-only* elements. Generally, the number of nodes and elements depends on the type of selected truss and number of modules.

The primary objective is to optimise the number of modules. Fig. 11 depicts the entire building. Each module comprises a truss beam with a

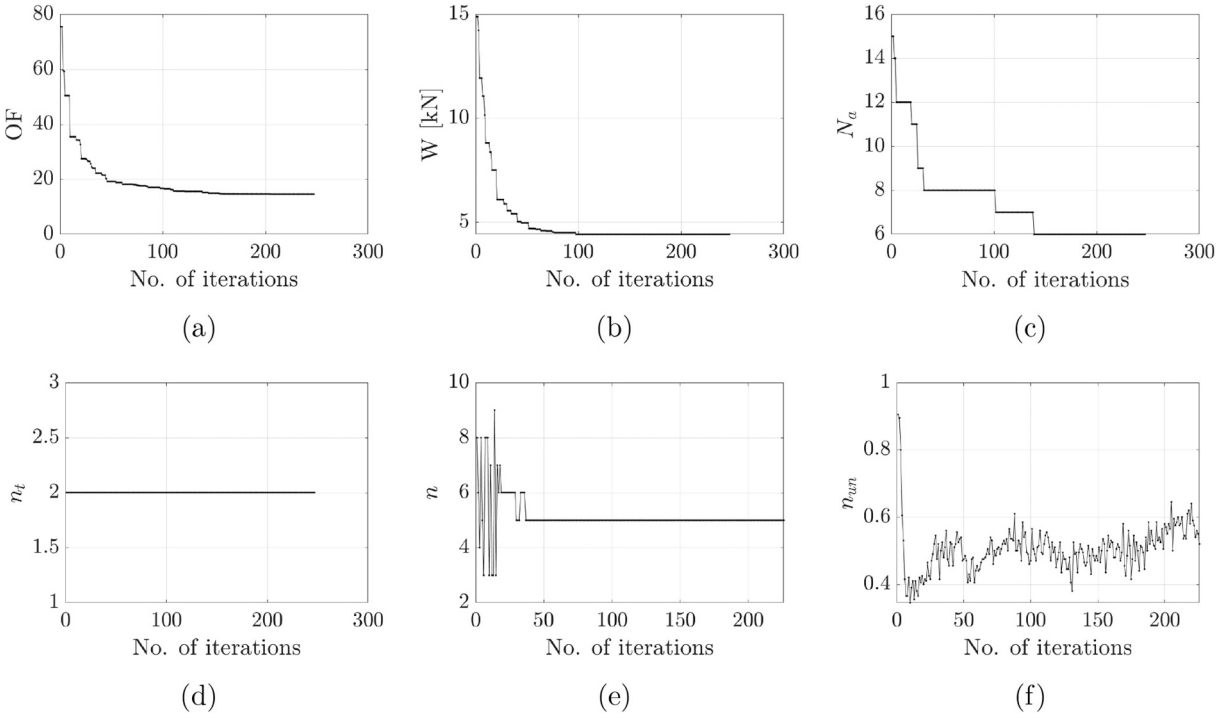

Fig. 10. Evolution of the (a) OF including penalties contributions, Objective function; (b) W, Weight of best individual excluding penalties contributions; (c) N_a, number of different class sections; (d) n_t, order number assigned for topology optimization; (e) n, number of subdivisions of half truss; (f) n_{un}, number of unfeasible members for the Case Study No.1.

Table 9
Results of the cases tested; in red, the parameters fixed in the size analyses.

Optimization case	Best OF	W [kN]	N_a	n	$H_1[m]$	$H_2[m]$	n_1	n_2	n_3
Size - case **A**: ϕ_1	4.162	4.162	12	6	1.33	2.5	2	2	2
Size - case **B**: $\phi_1+\phi_2$	9.748	5.156	4	6	1.33	2.5	2	2	2
Size & Shape - Case **A**: ϕ_1	4.399	4.399	10	7	1.33	1.59	1	1	5
Size & Shape - Case **B**: $\phi_1+\phi_2$	10.082	4.889	5	7	1.33	1.72	1	1	5
Size & Shape - Case **C**: $\phi_1+\phi_3$	6.148	4.224	11	5	1.33	1.81	1	1	3
Size & Shape - Case **D**: $\phi_1+\phi_2+\phi_3$	12.886	4.293	5	5	1.39	2.28	1	1	3
Size, Shape & Topology: $\phi_1+\phi_2+\phi_3$	12.429	4.363	5	4	1.7	2.38	1	1	2

Howe layout, supported by two steel columns. Except for the columns, which are securely anchored in the basement, and the vertical and horizontal bracings, assumed to be rigidly connected to the trusses and columns, respectively, all steel members, including purlins with the main trusses and truss elements, are designed to withstand axial stress. The column height is fixed at 5 m, and hinge-joints are strategically placed at the upper chord nodes of the truss for added stability. Additionally, the final design of the columns has been obtained from an inertial equivalence procedure performed due to the fact that Karamba3D does not allow structural verifications of coupled sections. Therefore, an equivalence in terms of total weight has been conducted in order to obtain a faithful estimation of the structural mass (refers to Fig. 11-(b).

Therefore, by fixing the overall length of the structure to 60 m, the distribution of modules can vary from being denser to more widely spaced. The final model consists of the following components:

- Truss system, categorized into the five components (i.e., Lower Chord, Upper Chord, Internal Vertical Struts, Upward-Downward Diagonals, Downward-Upward Diagonals);
- Columns;
- Purlins or Secondary beams, providing support for the roof;
- Roof bracings, positioned at the roof level;
- Vertical bracings type 1, located between the upper and bottom chords;
- Vertical bracings type 2, positioned between two consecutive frames.

In Fig. 12, each structure component is represented by a distinct colour, as indicated in the legend. Consequently, the lower and upper bounds for the parameter N_m are defined as follows:

$$3 < N_m < 8 \tag{14}$$

Based on the symmetric condition derived from:

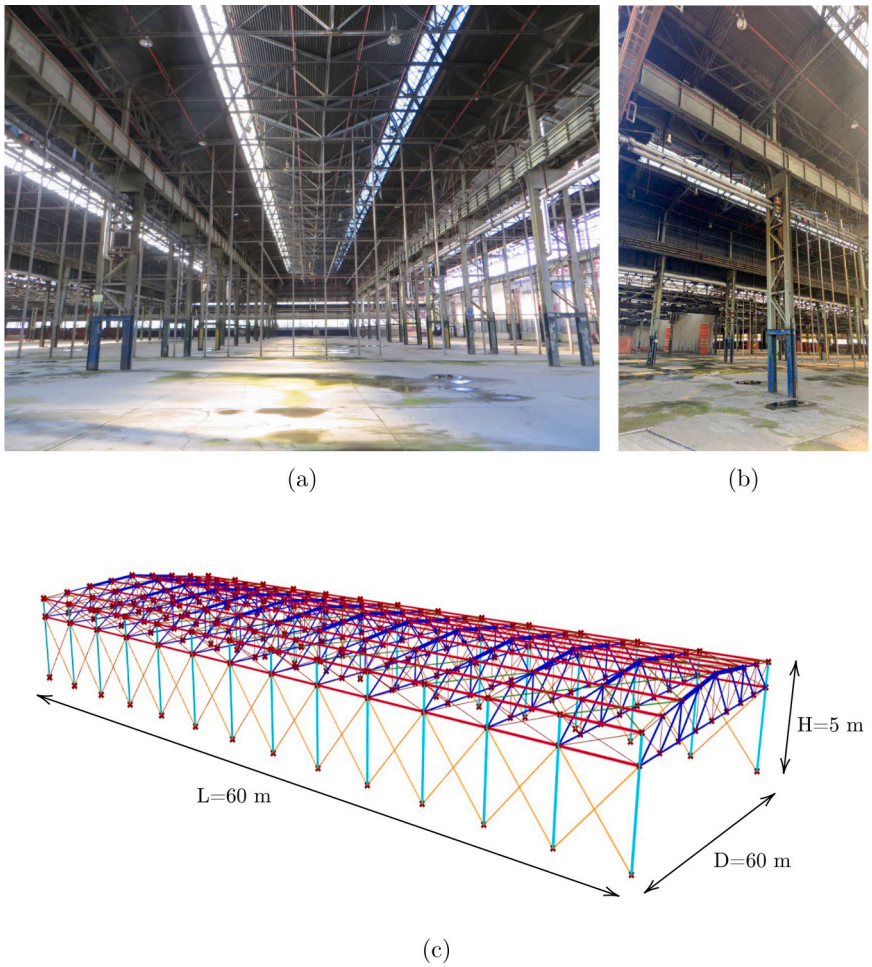

Fig. 11. (a) Internal view and (b) structural model of the considered industrial building.

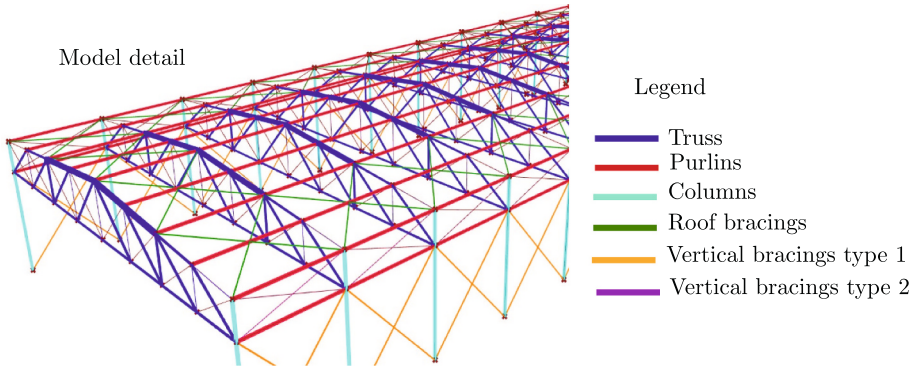

Fig. 12. Structural components of the industrial building.

$$\frac{L}{2}-\frac{s}{2}=(N_m-1)\cdot s \tag{15}$$

which leads to

$$N_m=\frac{\frac{L+s}{2}}{s};s=\frac{\frac{L}{2}}{N_m-\frac{1}{2}} \tag{16}$$

For clarity purposes, the layout configuration related to the lower bound has been reported in Fig. 13.

The structural analysis covers both vertical and lateral loads. Vertical loads encompass the Permanent Structural or Dead Load (G_1), representing the self-weight of all structural components, and the Permanent Non-Structural Load (G_2), which accounts for the weight of standard corrugated sheets commonly used for industrial building roofs. A weight of 0.05 kN/m^2 is assumed for these sheets. Additionally, the Maintenance Load (q_k) is determined based on the roof category, following Italian regulations, and is set at 0.4 kN/m^2, in line with Eurocode recommendations for roofs accessible solely for maintenance. The Snow Load (q_s) is calculated considering various factors, including exposure class, building location, shape coefficient, and thermal effects. This calculation results in a snow load of 1.23 kN/m^2. The effect of these loads on the truss elements as well as vertical supports, purlins, and vertical and horizontal bracings depends on the design variable n and varies dynamically between iterations as determined by the value of N_m.

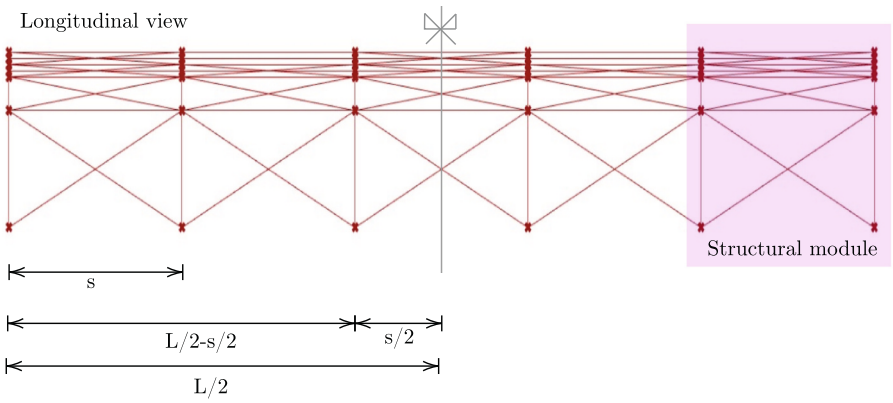

Fig. 13. Longitudinal view of the industrial building showing the main variables affecting the number of modules (N_m).

Lateral loads primarily consist of the Wind Load (p_w), which arises from aerodynamic forces due to the fluctuating velocity field of wind over time and space. It exerts lateral pressure on the external surfaces of large-span buildings. The Eurocode 1 recommends consulting the National Annex to determine wind pressure. The authors employed the Italian Standard Regulation NTC2018 in this study to assess the reference wind load. This approach considers factors such as the exposure coefficient, roughness class, and shape coefficient based on the building's location. It is important to note that each building facade experiences both positive (upwind wall) and negative (downwind wall) wind pressures, as well as ascending (upwind) and descending (downwind) pressures on the roof. For detailed wind action values (p_w) on each horizontal (roof) or vertical (facade) surface and their respective influence areas, refer to Table 10.

It is important to note that our analysis accounts not only for external pressures but also internal ones. The final combination has been chosen consistently to the most critical combination derived by adopting an envelope of all the possible load configurations. Referring to the ULS Eq. 11 and the corresponding amplification factor, γ, suggested by the Italian regulations, an overview of the adopted actions for the evaluation of the critical combination has been reported in Table 11:

4.2. Definition of the design variables

The optimization process applied to the industrial building follows the same objective function (Eq. 1) employed for the truss beams. Additionally, the same penalty approach utilizing three different penalties, ϕ_1, ϕ_2, and ϕ_3, has been implemented. In this adaptation, the concept of the number of sections (N_a) and the total number of pieces (N_{tot}) to encompass the new Design Variables (DVs) has been extended. Specifically, when calculating the value of N_{tot}, all elements comprising the entire structure have been considered, including the number of truss subdivisions (n) of the lower or upper chord halves (e.g. exploiting symmetry) for each truss beam within every frame and the total number of columns (N_{col}).

As a result, an expanded set of DVs has been introduced, bringing the total number of structural parameters to 27, as detailed in Table 12, showing only the new variables in addition to those in Table 4. This table also clearly indicates the chosen cross-section type for each structural element, ensuring compatibility between different profiles and offering feasible engineering solutions.

Moreover, six additional DVs have been integrated, encompassing column, purlin, horizontal bracing (roof) cross-sections, and two vertical bracings (facade) types. These new DVs complement the ones defined in the previous case study, as shown in Table 4. Furthermore, a shape-related DV has been introduced, the number of modules (N_m), which pertains to half of the structure's spatial configuration.

It is important to emphasize that the size, shape, and topology optimization conducted at the truss beam level work in tandem with the optimization of size and shape at the larger scale of the industrial building. While minimizing the cross-sections of the additional elements to meet structural requirements, the spacing between modules is dynamically adjusted during each iteration. In simpler terms, shape optimization at the industrial building level involves solely manipulating the number of modules, resulting in the removal or addition of trussed frames to the entire structure.

Table 10
Wind pressure p_w values for the different $c_p e$.

Structural element	c_p	p_w [KN/m^2]
Upwind wall	0.8	0.48
Downwind wall	−0.4	−0.24
Upwind roof pitch	−0.4	−0.24
Downwind roof pitch	−0.4	−0.24

Table 11
Summary of loads applied to the building and their relative value and coefficient.

Load Type	Load Name	Load Value [KN/m^2]	γ	ψ
Dead Load	G_1	Structure weight	1.3	–
Perm. Non-struct. Load	G2	0.05	1.5	–
Maintenance Load	q_k	0.5	1.5	–
Snow Load	q_s	1.23	1.5	0.5
Wind Load	p	Depends on c_p	1.5	0.6

Table 12
Design variables where the colors of the cells represent the different categories: purple - Global layout definition; orange - Additional size design variables.

Design variable	Description	Domain
x_{22}	Numbers of modules in one half	$3 \div 8$
x_{23}	Column HEA cross-section	$0 \div 23$ profiles' index from catalogue
x_{24}	Purlin IPE cross-section	$0 \div 17$ profiles' index from catalogue
x_{25}	Roof bracing ROD cross-section	$0 \div 24$ profiles' index from catalogue
x_{26}	Vertical bracing type 1 ROD cross-section	$0 \div 24$ profiles' index from catalogue
x_{27}	Vertical bracing type 2 ROD cross-section	$0 \div 24$ profiles' index from catalogue

4.3. Results

In this section, the authors summarise the optimization results for the industrial building. The analysis has been conducted 20 times to facilitate a comprehensive statistical examination of the solution dataset. Table 13 below showcases the results, organized in ascending order of the best OF values.

It is manifest that the Howe truss configuration is the optimizer's preferred choice in most runs. Furthermore, it consistently achieves the lowest OF values and, simultaneously, the lowest weight. This preference can be attributed to the Howe truss's suitability in handling the uplift effect caused by wind action, both externally and internally.

The impact of the adopted penalty approach becomes apparent when considering structural parameters related to complexity. The number of cross-sections (N_a) is often reduced to three for the best configurations (primarily Howe trusses). Additionally, the number of chords' subdivisions (n) for these designs is always minimized to four, independent of the configuration. This parameter indirectly influences the total number of pieces (N_{tot}) and modules (N_m). Especially for the last one, it is usually set to four, aligning with the need to reduce construction elements for safety and feasibility.

There is a notable variability in the geometric layout of the truss designs. The values of H_1 and H_2, representing truss beam heights at the edge and middle, respectively, vary within the ranges of 1.44 to 2 and 1.67 to 2.5. This variability demonstrates the adaptability of the optimization process in determining optimal geometries based on structural requirements.

While the Howe truss is preferred, other truss typologies like Warren and Pratt are occasionally selected but result in higher OF values and total weights. This suggests that these configurations might be less suitable for the given structural requirements and load conditions.

A visual representation of the optimal Howe truss, with each section distinguished by a unique colour, is presented in Fig. 14. Furthermore, Tables 14 and 15 provide a detailed breakdown of the cross-sections assigned to all structural members. It has been observed that the deflection limit always guided the cross-section assignments and constrained the overall layout of the building by reducing the longitudinal spans as well as the number of modules. However, the Demand-capacity ratio of the structural elements composing the truss is always over 65% while vertical supports, bracings, and purlins achieve almost 90%. It validates the optimized sizing achieved by the final design.

Table 16 displays the Best, Worst, Mean values, and the Standard Deviation of the OF from all 20 optimization runs.

Aiming to discuss the algorithm's capability to find the optimal solution and the goodness of the adopted penalty approach, the plot of the OF and total weight curve of the best design versus the number of iterations has been reported in Fig. 15.

Furthermore, valuable insights can be gained by examining the evolution of structural parameters, specifically N_a and n, during the optimization process. It's worth highlighting that while the optimal value for the number of different sections, N_a, was reached after approximately 200 iterations, the number of truss subdivisions, n, was fixed at four from the outset of the optimization process.

Table 13
Results of the best individual of each optimization for the Industrial building.

No. run	Best OF	Weight [kN]	N_a	n	H_1	H_2	n_1	n_2	n_3	N_m	Topology
1	775.427	330.228	3	4	2	2.17	1	1	2	7	Howe
2	790.020	336.442	3	4	2	2	1	1	2	5	Howe
3	885.230	339.024	4	4	2	2	2	1	1	5	Howe
4	888.228	340.172	4	4	1.99	2.07	1	1	1	6	Howe
5	894.320	342.505	4	4	1.99	2.01	1	1	1	5	Howe
6	940.256	350.687	4	4	1.67	1.75	1	2	1	5	Howe
7	932.095	396.947	3	4	1.94	2.01	2	1	1	6	Warren
8	937.174	399.110	3	4	2	2.43	1	1	1	5	Howe
9	940.256	350.687	4	4	1.67	1.75	1	2	1	5	Howe
10	941.401	400.910	3	4	1.46	1.57	1	2	1	5	Howe
11	964.094	369.228	4	4	1.54	1.64	1	1	1	6	Howe
12	967.429	370.505	4	4	1.67	1.67	2	1	1	6	Howe
13	971.380	372.018	4	4	1.75	1.78	2	1	1	8	Warren
14	974.337	341.988	5	4	2	2.1	2	1	1	5	Howe
15	983.096	376.505	4	4	1.87	1.95	1	1	1	8	Pratt
16	991.875	378.404	4	4	1.87	1.95	1	1	1	5	Howe
17	1014.911	356.229	5	4	1.68	1.87	1	2	1	5	Howe
18	1023.262	391.888	4	4	2	2.31	1	2	1	7	Warren
19	1036.499	396.957	4	4	2	2	1	2	1	7	Pratt
20	1042.326	399.189	4	4	1.96	2.16	1	1	1	6	Pratt

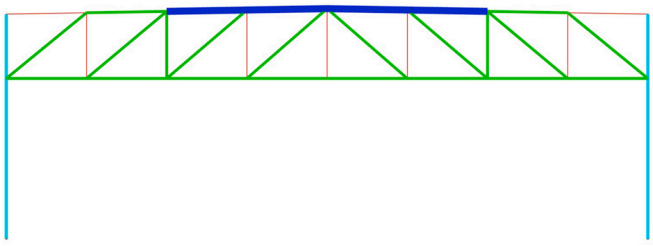

Fig. 14. Configuration of the Howe truss in the optimized Industrial building.

Table 14
Cross-sections of the optimized truss in the Industrial building.

Structural element	CHS First group	CHS Second group	CHS Third group
Lower Chord	88.9 × 2.5	88.9 × 2.5	88.9 × 2.5
Upper Chord	219.1 × 6	88.9 × 2.5	21.3 × 2
Int. Vert. Structs	21.3 × 2	88.9 × 2.5	21.3 × 2
Upward-Downward Diagonals	88.9 × 2.5	88.9 × 2.5	88.9 × 2.5

Table 15
Cross-sections of the structural elements in the Industrial building.

Structural Elements	Cross Section Type
Columns	HEA 100
Purlins	IPE 120
Roof Bracings	Circle 80
Vertical Bracings 1	Circle 65
Vertical Bracings 2	Circle 50

Table 16
Best, Worst, Mean and Standard deviation related to the OF values of the optimized Industrial building with Howe truss.

Best	Worst	Mean	Standard Deviation
775.427	1014.911	942.425	77.05

5. Conclusions

This paper presented an optimization framework for steel structures, ranging from truss beams to real-world inspired industrial buildings. The study leveraged a penalty-based optimization method, incorporating three distinct penalty functions (ϕ_1, ϕ_2, and ϕ_3) to address structural complexity while concurrently optimizing size, shape, and topology. The search for the optimal solution is conducted using an SPEA-II algorithm.

This approach demonstrated its efficacy in efficiently assigning cross-sections based on stress levels and refining structural sizing in truss beam optimization. Extending the investigation to industrial building design, the parallel influence of truss beam-level optimizations on a real-world inspired industrial building has been observed. The optimization process successfully minimized cross-sections for additional elements, such as columns and bracings, while dynamically adjusting the number of modules within the building. The results showcased a preference for

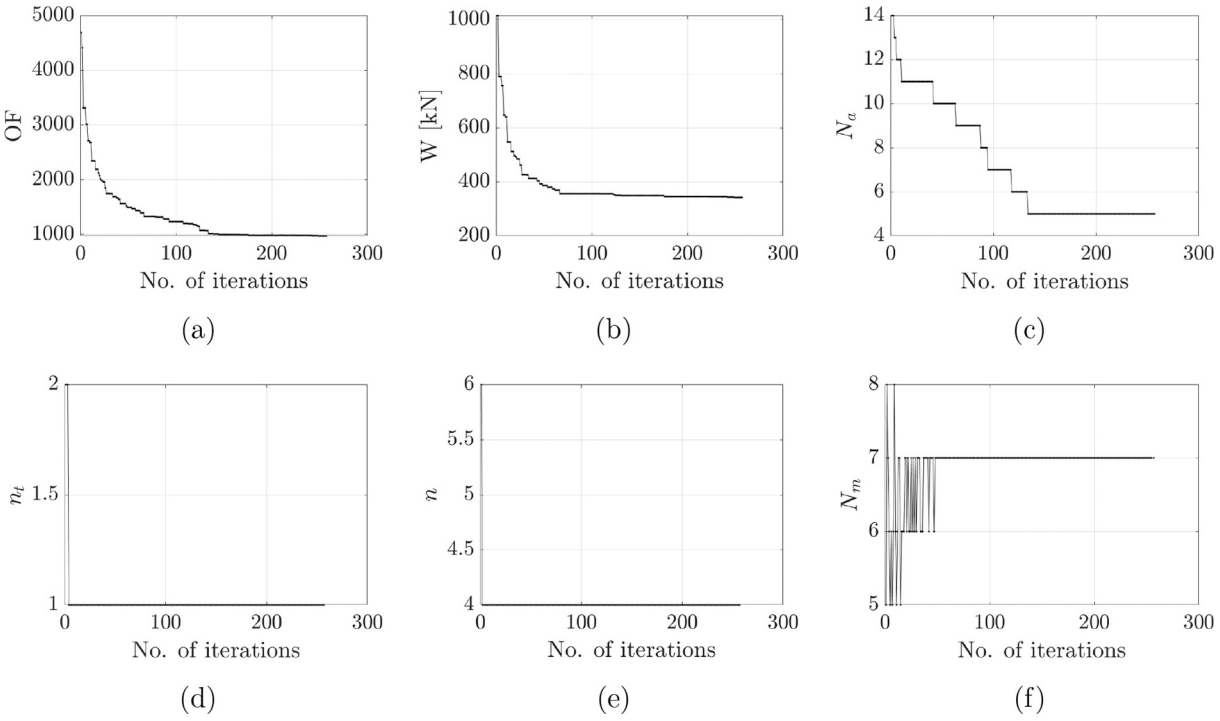

Fig. 15. Evolution of the (a) OF, Objective function; (b) W, Weight of best individual; (c) N_a, number of different class sections; (d) n_t, order number assigned for topology optimization; (e) n, number of subdivisions of half truss; (f) n_{un}, number of unfeasible members for the Case study No.2.

the Howe truss configuration, which emerged as the most efficient choice in terms of both overall function (OF) and weight. The paper also provided insights into the dynamic evolution of key structural parameters during optimization. Notably, the number of different cross-sections (N_a) exhibited a steady convergence trend, while the number of subdivisions of half truss (n) quickly stabilized.

In conclusion, the proposed optimization approach, driven by penalty functions and adaptive cross-section assignments, offers a robust and flexible framework for designing steel structures. The successful application to truss beams and industrial buildings demonstrates its versatility and efficiency in managing complexity, reducing weight, and ensuring structural integrity. This research contributes to advancing structural optimization methods, with practical implications for cost-effective and sustainable construction practices in various engineering applications. Further developments of the work will explore additional complexities and real-world constraints to refine and expand the applicability of this approach in structural engineering and design. Specifically, structural complexity will be investigated at the level of the connections of critical infrastructures (i.e. steel or steel-concrete composite bridge) where the standardization of structural joints plays a crucial role, leading to significant time and economic cost savings because of the simplification at the design and construction processes.

CRediT authorship contribution statement

Raffaele Cucuzza: Writing – review & editing, Writing – original draft, Visualization, Validation, Supervision, Software, Methodology, Investigation, Formal analysis, Data curation, Conceptualization. **Angelo Aloisio:** Writing – review & editing, Writing – original draft, Visualization, Validation, Data curation. **Majid Movahedi Rad:** Writing – review & editing, Visualization, Validation, Supervision, Investigation. **Marco Domaneschi:** Writing – review & editing, Visualization, Resources, Investigation, Funding acquisition.

Declaration of competing interest

The authors declare no competing financial interests or personal relationships that could have appeared to influence the work reported in this paper.

Data availability

All data, models, or codes supporting this study's findings are available from the corresponding author upon request.

Acknowledgements

The authors are grateful to Maffeis Engineering S.p.A. for sharing valuable information about the practical design of truss structures and steel buildings. Eng.s Arianna Zamagna and Antonio Sforza are also acknowledged for the support given during the modelling phase into the Grasshopper environment.

Therefore, the research leading to these results has received funding from (i) the European Research Council under the Grant agreement ID: 101007595 of the project ADDOPTML, MSCA RISE 2020 Marie Skodowska Curie Research and Innovation Staff Exchange (RISE); (ii) the European Union HORIZON-MSCA-2021-SE-01, grant agreement No: 101086413, ReCharged - Climate-aware Resilience for Sustainable Critical and interdependent Infrastructure Systems enhanced by emerging Digital Technologies.

Appendix A

In this section, a comparison between the adopted optimisation algorithm SPEA-II and other well-known metaheuristic search techniques has been pointed out. The effectiveness and robustness of SPEA-II as well as the goodness of the results obtained from the investigated case studies, in terms of

numerical correctness, efficiency and validation, will be demonstrated. To achieve this goal, 10-bar cantilever truss and 25-bar space truss have been selected as structures widely used in structural optimisation to verify design approaches and compare different numerical techniques. This structure has been previously studied for discrete design variables by Rajeev and Krishnamoorthy [99] using Genetic Algorithm (GA), Kripka [100] using Simulated Annealing (SA), Camp and Bichon [101] using Ant Colony Optimization (ACO), and Sonmez [102] using Artificial Bee Colony (ABC) algorithm

For the truss layout definition of the conducted numerical tests as well as element numbers and DVs assignation, material properties, discrete cross-section catalogue, and boundary and loading conditions, the authors referred to [102]. For both the examples presented in this appendix, the SPEA-II algorithm parameters were set as reported in the Table A.17. In order to test the convergence capability of the algorithm, the authors coherently have been adopted similar parameters' settings assumed for case studies No.1 and No.2. Additionally, only penalty ϕ_1 for minimum weight has been implemented making the results comparable with those obtained for the other algorithms.

Table A.17: Optimization algorithm parameters and settings.

Parameter	Value
Maximum Iterations	100
Population Size	100
Mutation Probability	0.05
Crossover Probability	0.7
Convergence Threshold	0.001
Selection Mechanism	Tournament Selection
Penalty Functions	ϕ_1
No. of independent runs	20
Algorithm Integration	SPEA-II (Octopus Plugin)

Table A.18 and A.19 list the best design developed by SPEA-II in comparison with all the selected algorithms. Additionally, the main numerical features like the best solution, the average among all the runs, the worst design, the total number of evaluations for each run, and the eventual constraint violation have been pointed out. As expected, if for the 10-bar truss the SPEA-II performs better than GA algorithm either in terms of least weight and standard deviation, the best design is achieved with a higher least weight with respect to SA, ACO and ABC algorithms. On the other hand, the computational effort expressed by the number of evaluations is one of the lowest among the tested optimisation strategies. Moving on to the second numerical benchmark, the SPEA-II and GA achieved the same best design providing the same optimal cross-section assignation. However, as in the previous case, SA, ACO, and ABC algorithms performed better although less required computational effort.

Table A.18: Optimization results for the 10-bar truss.

Variables		Optimal cross-section area ($in.^2$)				
No	Des.Var.	GA	SA	ACO	ABC	This study
1	A_1	33.50	33.50	33.50	33.50	30.00
2	A_2	1.62	1.62	1.62	1.62	1.8
3	A_3	22.00	22.90	22.90	22.90	26.5
4	A_4	15.50	14.20	14.20	14.20	16.00
5	A_5	1.62	1.62	1.62	1.62	1.62
6	A_6	1.62	1.62	1.62	1.62	1.62
7	A_7	14.20	7.97	7.97	7.97	11.5
8	A_8	19.90	22.90	22.90	22.90	18.8
9	A_9	19.90	22.00	22.00	22.00	22.00
10	A_{10}	2.62	1.62	1.62	1.62	1.8
Best (lb)		5613.84	5490.74	5490.74	5490.74	5545.76
Average (lb)		N/A	N/A	N/A	5510.35	5515.76
Worst (lb)		N/A	N/A	N/A	5536.97	5736.97
Evaluation (#)		N/A	N/A	10,000	25,800	10,000
Constraint violation		None	None	None	None	None

Table A.19: Optimisation results for the 25-bar truss.

Variables		Optimal cross-section area ($in.^2$)				
No	Des.Var.	GA	SA	ACO	ABC	This study
1	A_1	0.1	0.1	0.1	0.1	0.1
2	$A_2 \sim A_5$	1.8	0.4	0.3	0.3	1.8
3	$A_6 \sim A_9$	2.3	3.4	3.4	3.4	2.3
4	$A_{10} \sim A_{11}$	0.2	0.1	0.1	0.1	0.2
5	$A_{12} \sim A_{13}$	0.1	2.2	2.1	2.1	0.1
6	$A_{14} \sim A_{17}$	0.8	1.0	1.0	1.0	0.8
7	$A_{18} \sim A_{21}$	1.8	0.4	0.5	0.5	1.8
8	$A_{22} \sim A_{25}$	3.0	3.4	3.4	3.4	3.0
Best (lb)		546.010	484.330	484.85	484.85	546.010
Average (lb)		N/A	N/A	N/A	486.46	560.46
Worst (lb)		N/A	N/A	N/A	486.46	586.010
Evaluation (#)		840	40,000	7700	25,250	10,000
Constraint violation		None	None	None	None	None

Finally, even if the SPEA-II algorithm does not represent the best strategy already developed in Literature, it assures a good level of efficiency and robustness for this specific class of single-objective optimisation problem coherently with the computational effort and structural complexity required by 2D and 3D truss systems employed, as case studies, in this research.

References

[1] M. Akhani, A. Kashani, M. Mousavi, A. Gandomi, A hybrid computational intelligence approach to predict spectral acceleration, Measure.: J. Intern. Measure. Confeder. 138 (2019) 578–589, https://doi.org/10.1016/j.measurement.2019.02.054.

[2] M.M. Rosso, R. Cucuzza, G.C. Marano, A. Aloisio, G. Cirrincione, Review on deep learning in structural health monitoring, in: Bridge Safety, Maintenance, Management, Life-Cycle, Resilience and Sustainability, CRC Press, 2022, pp. 309–315, https://doi.org/10.1201/9781003322641-34.

[3] M.M. Rosso, A. Aloisio, R. Cucuzza, D.P. Pasca, G. Cirrincione, G.C. Marano, Structural health monitoring with artificial neural network and subspace-based damage indicators, in: A. Gomes Correia, M. Azenha, P.J.S. Cruz, P. Novais, P. Pereira (Eds.), Trends on Construction in the Digital Era, Springer International Publishing, Cham, 2023, pp. 524–537.

[4] P. Aminian, M. Javid, A. Asghari, A. Gandomi, M. Arab Esmaeili, A robust predictive model for base shear of steel frame structures using a hybrid genetic programming and simulated annealing method, Neural Comput. & Applic. 20 (2011) 1321–1332, https://doi.org/10.1007/s00521-011-0689-0.

[5] M. Zabihi-Samani, Design of optimal slit steel damper under cyclic loading for special moment frame by cuckoo search, Int. J. Steel Struct. 19 (4) (2019) 1260–1271, https://doi.org/10.1007/s13296-019-00206-6.

[6] V. Shafaie, O. Ghodousian, A. Ghodousian, R. Cucuzza, M.M. Rad, Integrating push-out test validation and fuzzy logic for bond strength study of fiber-reinforced self-compacting concrete, Constr. Build. Mater. 425 (2024) 136062, https://doi.org/10.1016/j.conbuildmat.2024.136062.

[7] H. Long, H. Nguyen Dang, J.-P. Jaspart, J.-F. Demonceau, An overview of the plastic-hinge analysis of 3d steel frames, Asia Pac. J. Comput. Eng. 2 (2015), https://doi.org/10.1186/s40540-015-0016-9.

[8] S. Zhang, Y.H. Chui, Characterizing flexural behaviour of panel-to-panel connections in cross-laminated timber floor systems, Structures 28 (2020) 2047–2055, https://doi.org/10.1016/j.istruc.2020.10.040.

[9] S. Boonstra, K. van der Blom, H. Hofmeyer, M.T. Emmerich, Hybridization of an evolutionary algorithm and simulations of co-evolutionary design processes for early-stage building spatial design optimization, Autom. Constr. 124 (2021) 103522, https://doi.org/10.1016/j.autcon.2020.103522.

[10] M. Habashneh, R. Cucuzza, M. Domaneschi, M. Movahedi Rad, Advanced elasto-plastic topology optimization of steel beams under elevated temperatures, Adv. Eng. Softw. 190 (2024) 103596, https://doi.org/10.1016/j.advengsoft.2024.103596.

[11] A. Kashani, C. Camp, M. Rostamian, K. Azizi, A. Gandomi, Population-based optimization in structural engineering: a review, Artif. Intell. Rev. 55 (2021) 1–108, https://doi.org/10.1007/s10462-021-10036-w.

[12] M. Abdel-Basset, L. Abdel-Fatah, A. Sangaiah, Metaheuristic Algorithms: A Comprehensive Review, 2018, https://doi.org/10.1016/B978-0-12-813314-9.00010-4.

[13] T. Dokeroglu, E. Sevinc, T. Kucukyilmaz, A. Cosar, A survey on new generation metaheuristic algorithms, Comput. Ind. Eng. 137 (2019), https://doi.org/10.1016/j.cie.2019.106040.

[14] L. Abualigah, D. Yousri, M. Abd Elaziz, A. Ewees, M. Al-qaness, A. Gandomi, Aquila optimizer: a novel meta-heuristic optimization algorithm, Comput. Ind. Eng. 157 (2021) 2087–2098, https://doi.org/10.1016/j.cie.2021.107250.

[15] R. Cucuzza, M. Domaneschi, R. Greco, G.C. Marano, Numerical models comparison for fluid-viscous dampers: performance investigations through genetic algorithm, Comput. Struct. 288 (2023) 107122, https://doi.org/10.1016/j.compstruc.2023.107122.

[16] M. Kashani, J. Maddocks, E. Afsar Dizaj, Residual capacity of corroded reinforced concrete bridge components: a state-of-the-art review, J. Bridg. Eng. 24 (2019), https://doi.org/10.1061/(ASCE)BE.1943-5592.0001429), 03119001–1.

[17] Z. Gao, X. Zhang, Y. Wang, R. Yang, G. Wang, Z. Wang, Measurement of the poisson's ratio of materials based on the bending mode of the cantilever plate, BioResources 11 (3) (2016) 5703–5721, https://doi.org/10.15376/biores.11.3.5703-5721.

[18] G. Bekdaş, S. Nigdeli, A. Kayabekir, X.-S. Yang, Optimization in Civil Engineering and Metaheuristic Algorithms: A Review of State-of-the-art Developments, 2018, https://doi.org/10.1007/978-3-319-96433-1_6.

[19] A.H. Gandomi, S. Talatahari, X.-S. Yang, S. Deb, Design optimization of truss structures using cuckoo search algorithm, Struct. Design Tall Spec. Build. 22 (17) (2013) 1330–1349, https://doi.org/10.1002/tal.1033.

[20] A. Gandomi, A. Kashani, M. Mousavi, M. Jalalvandi, Slope stability analyzing using recent swarm intelligence techniques, Int. J. Numer. Anal. Methods Geomech. 39 (2014) 295–309, https://doi.org/10.1002/nag.2308.

[21] A. Gandomi, X.-S. Yang, S. Talatahari, A. Alavi, Metaheuristic Algorithms in Modeling and Optimization, 2013, pp. 1–24, https://doi.org/10.1016/B978-0-12-398364-0.00001-2.

[22] B. Topping, Shape optimization of skeletal structures: a review, J. Struct. Eng. (U. S.) 109 (8) (1983) 1933–1951, https://doi.org/10.1061/(ASCE)0733-9445(1983)109:8(1933).

[23] A. Horn, Integrating Constructability into Conceptual Structural Design and Optimization, Ph.D. thesis, Massachusetts Institute of Technology, 2015. accessed: July 9, 2024. URL, http://digitalstructures.mit.edu/.

[24] S.-W. Jin, H. Ohmori, S.-J. Lee, Optimal design of steel structures considering welding cost and constructability of beam-column connections, J. Constr. Steel Res. 135 (2017) 292–301, https://doi.org/10.1016/j.jcsr.2017.03.020.

[25] R. Cucuzza, C. Costi, M.M. Rosso, M. Domaneschi, G.C. Marano, D. Masera, Optimal strengthening by steel truss arches in prestressed girder bridges, in: Proceedings of the Institution of Civil Engineers-Bridge Engineering, 2021, pp. 1–21, https://doi.org/10.1680/jbren.21.00056.

[26] M.M. Rosso, R. Cucuzza, A. Aloisio, G.C. Marano, Enhanced multi-strategy particle swarm optimization for constrained problems with an evolutionary-strategies-based unfeasible local search operator, Appl. Sci. 12 (5) (2022), https://doi.org/10.3390/app12052285.

[27] M.M. Rosso, R. Cucuzza, F. Di Trapani, G.C. Marano, Nonpenalty machine learning constraint handling using pso-svm for structural optimization, Adv. Civ. Eng. 2021 (2021), https://doi.org/10.1155/2021/6617750.

[28] M.M. Rosso, A. Aloisio, R. Cucuzza, R. Asso, G.C. Marano, Structural optimization with the multistrategy pso-es unfeasible local search operator, in: Proceedings of International Conference on Data Science and Applications: ICDSA 2022 1, 2023, pp. 215–229, https://doi.org/10.1007/978-981-19-6631-616.

[29] W.W. Hager, D.W. Hearn, P.M. Pardalos, Large Scale Optimization: State of the Art, Springer Science & Business Media, 2013, https://doi.org/10.1007/978-1-4613-3632-7.

[30] F.K. Jawad, M. Mahmood, D. Wang, O. Al-Azzawi, A. Al-Jamely, Heuristic dragonfly algorithm for optimal design of truss structures with discrete variables 29 (2021) 843–862, https://doi.org/10.1016/j.istruc.2020.11.071.

[31] L.-J. Li, Z. Huang, F. Liu, Q. Wu, A heuristic particle swarm optimizer for optimization of pin connected structures, Comput. Struct. 85 (7–8) (2007) 340–349, https://doi.org/10.1016/j.compstruc.2006.11.020.

[32] R.H. Byrd, S.L. Hansen, J. Nocedal, Y. Singer, A stochastic quasi-newton method for large-scale optimization, SIAM J. Optim. 26 (2) (2016) 1008–1031, https://doi.org/10.48550/arXiv.1401.7020.

[33] R. Cheng, Y. Jin, A competitive swarm optimizer for large scale optimization, IEEE Transact. Cybernet. 45 (2) (2014) 191–204, https://doi.org/10.1109/TCYB.2014.2322602.

[34] S. Kazemzadeh Azad, S. Kazemzadeh Azad, A standard benchmarking suite for structural optimization algorithms: Iscso 2016–2022 58 (2023) 105409, https://doi.org/10.1016/j.istruc.2023.105409.

[35] A.H. Gandomi, X.-S. Yang, Benchmark problems in structural optimization, in: S. Koziel, X.-S. Yang (Eds.), Computational Optimization, Methods and Algorithms, Springer, Berlin Heidelberg, Berlin, Heidelberg, 2011, pp. 259–281, https://doi.org/10.1007/978-3-642-20859-112.

[36] S.-J. Wu, P.-T. Chow, Integrated discrete and configuration optimization of trusses using genetic algorithms, Comput. Struct. 55 (1995) 695–702, https://doi.org/10.1016/0045-7949(94)00426-4.

[37] C.-K. Soh, J.-P. Yang, Optimal layout of bridge trusses by genetic algorithms, Comput. Aided Civ. Inf. Eng. 13 (1998) 247–254, https://doi.org/10.1111/0885-9507.00103.

[38] A. Kaveh, S. Talatahari, An enhanced charged system search for configuration optimization using the concept of fields of forces, Struct. Multidiscip. Optim. 43 (2010) 339–351, https://doi.org/10.1007/s00158-010-0571-1.

[39] L.F.F. Miguel, L.F.F. Miguel, Shape and size optimization of truss structures considering dynamic constraints through modern metaheuristic algorithms, Expert Syst. Appl. 39 (2012) 9458–9467, https://doi.org/10.1016/j.eswa.2012.02.113.

[40] S. Kazemzadeh Azad, M. Bybordiani, S. Kazemzadeh Azad, F. Jawad, Simultaneous size and geometry optimization of steel trusses subjected to dynamic excitations, Struct. Multidiscip. Optim. 58 (2018) 2545–2563, https://doi.org/10.1007/s00158-018-2039-7.

[41] V.-H. Truong, S. Tangaramvong, G. Papazafeiropoulos, An efficient lightgbm-based differential evolution method for nonlinear inelastic truss optimization, Expert Syst. Appl. 237 (2024) 121530, https://doi.org/10.2139/ssrn.4395575.

[42] M. Madhav, N. Kameswara Rao, K. Madhavan, Laterally loaded pile in elasto-plastic soil, Soils Found. 11 (2) (1971) 1–15, https://doi.org/10.3208/sandf1960.11.21.

[43] I. Hajirasouliha, K. Pilakoutas, H. Moghaddam, Topology optimization for the seismic design of truss-like structures, Comput. Struct. 89 (7–8) (2011) 702–711, cited By 43, https://doi.org/10.1016/j.compstruc.2011.02.003.

[44] K. Li, L. Pan, W. Xue, H. Jiang, H. Mao, Multi-objective optimization for energy performance improvement of residential buildings: a comparative study, Energies 10 (2) (2017) 245, https://doi.org/10.3390/en10020245.

[45] V.-H. Truong, S.-E. Kim, A robust method for optimization of semi-rigid steel frames subject to seismic loading, J. Constr. Steel Res. 145 (2018) 184–195, https://doi.org/10.1016/j.jcsr.2018.02.025.

[46] J.S. Russell, K.E. Swiggum, J.M. Shapiro, A.F. Alaydrus, Constructability related to tqm, value engineering, and cost/benefits, J. Perform. Constr. Facil. 8 (1) (1994) 31–45, https://doi.org/10.1061/(ASCE)0887-3828(1994)8:1(31).

[47] M. Hayalioglu, S. Degertekin, Minimum cost design of steel frames with semi-rigid connections and column bases via genetic optimization, Comput. Struct. 83 (21−22) (2005) 1849–1863, https://doi.org/10.1016/j.compstruc.2005.02.009.
[48] D. Arditi, A. Elhassan, Y.C. Toklu, Constructability analysis in the design firm, J. Constr. Eng. Manag. 128 (2) (2002) 117–126, https://doi.org/10.1061/(ASCE)0733-9364(2002)128:2(117).
[49] S. Anderson, D. Fisher, V. Gupta, Total Constructability Management: A Process-Oriented Framework, Project Management Institute, 1995.
[50] J.T. O'Connor, S.E. Rusch, M.J. Schulz, Constructability concepts for engineering and procurement, J. Constr. Eng. Manag. 113 (2) (1987) 235–248, https://doi.org/10.1061/(ASCE)0733-9364(1987)113:2(235.
[51] M.H. Pulaski, M.J. Horman, Organizing constructability knowledge for design, J. Constr. Eng. Manag. 131 (8) (2005) 911–919, https://doi.org/10.1061/(ASCE)0733-9364(2005)131:8(911).
[52] S. Khan, Constructability: A Tool for Project Management, CRC Press, 2018. ISBN 9780367606862.
[53] B. Paulson Jr., Designing to reduce construction costs, J. Constr. Div. 102 (C04) (1976), https://doi.org/10.1061/JCCEAZ.0000639.
[54] D.I. Ruby, Constructability of Structural Steel Buildings, American Institute of Steel Construction, 2008.
[55] J.A. Gambatese, J.B. Pocock, P.S. Dunston, Constructability Concepts and Practice, American Society of Civil Engineers, 2007. ISBN (print):978-0-7844-0895-7.
[56] A. Xu, S. Li, J. Fu, A. Misra, R. Zhao, A hybrid method for optimization of frame structures with good constructability, Eng. Struct. 276 (2023) 115338, https://doi.org/10.1016/j.engstruct.2022.115338.
[57] C. Pasquire, A. Gibb, Considerations for assessing the benefits of standardisation and pre-assembly in construction (the findings of a pilot study), in: Report to CIBSE Seminar on Standardisation in the Design and Construction of Building Services Installations Vol. 26, 1999.
[58] F.W. Wong, P.T. Lam, E.H. Chan, F.K. Wong, Factors affecting buildability of building designs, Can. J. Civ. Eng. 33 (7) (2006) 795–806, https://doi.org/10.1139/L06-022.
[59] F.W. Wong, P.T. Lam, E.H. Chan, L. Shen, A study of measures to improve constructability, Intern. J. Qual. Reliabil. Manage. 24 (6) (2007) 586–601, https://doi.org/10.1108/02656710710757781.
[60] R. Walls, A. Elvin, An algorithm for grouping members in a structure, Eng. Struct. 32 (6) (2010) 1760–1768, https://doi.org/10.1016/j.engstruct.2010.02.027.
[61] Y. Deng, Y. Liu, D. Zhou, An improved genetic algorithm with initial population strategy for symmetric tsp, Math. Probl. Eng. 2015 (1) (2015) 212794, https://doi.org/10.1155/2015/212794.
[62] J.P.G. Carvalho, D.E. Vargas, B.P. Jacob, B.S. Lima, P.H. Hallak, A.C. Lemonge, Multi-objective structural optimization for the automatic member grouping of truss structures using evolutionary algorithms, Comput. Struct. 292 (2024) 107230, https://doi.org/10.1016/j.compstruc.2023.107230.
[63] C. Provatidis, D. Venetsanos, Cost minimization of 2d continuum structures under stress constraints by increasing commonality in their skeletal equivalents, Forsch. Ingenieurwes. 70 (3) (2006) 159–169, https://doi.org/10.1007/s10010-006-0026-4.
[64] V. Toğan, A.T. Daloğlu, An improved genetic algorithm with initial population strategy and self-adaptive member grouping, Comput. Struct. 86 (11−12) (2008) 1204–1218, https://doi.org/10.1016/j.compstruc.2007.11.006.
[65] J. Biedermann, D. Grierson, Training and using neural networks to represent heuristic design knowledge, Adv. Eng. Softw. 27 (1–2) (1996) 117–128, https://doi.org/10.1016/0965-9978(96)00017-8.
[66] T.R. van Woudenberg, F.P. van Der Meer, A grouping method for optimization of steel skeletal structures by applying a combinatorial search algorithm based on a fully stressed design, Eng. Struct. 249 (2021) 113299, https://doi.org/10.1016/j.engstruct.2021.113299.
[67] M. Mashayekhi, E. Salajegheh, M. Dehghani, Topology optimization of double and triple layer grid structures using a modified gravitational harmony search algorithm with efficient member grouping strategy, Comput. Struct. 172 (2016) 40–58, https://doi.org/10.1016/j.compstruc.2016.05.008.
[68] H.J. Barbosa, A.C. Lemonge, C.C. Borges, A genetic algorithm encoding for cardinality constraints and automatic variable linking in structural optimization, Eng. Struct. 30 (12) (2008) 3708–3723, https://doi.org/10.1016/j.engstruct.2008.06.014.
[69] K. Shea, J. Cagan, S.J. Fenves, A shape annealing approach to optimal truss design with dynamic grouping of members, J. Mech. Des. 119 (3) (1997) 388–394, https://doi.org/10.1115/1.2826360.
[70] M. Galante, Genetic algorithms as an approach to optimize real-world trusses, Int. J. Numer. Methods Eng. 39 (3) (1996) 361–382, https://doi.org/10.1002/(SICI)1097-0207.
[71] F.Y. Kocer, J.S. Arora, Standardization of steel pole design using discrete optimization, J. Struct. Eng. 123 (3) (1997) 345–349, https://doi.org/10.1061/(ASCE)0733-9445(1997)123:3(345.
[72] S. Kazemzadeh Azad, S. Aminbakhsh, S.S. Shaban, Multi-stage guided stochastic search for optimization and standardization of free-form steel double-layer grids 34 (2021) 678–699, https://doi.org/10.1016/j.istruc.2021.07.068.
[73] M. Hayalioglu, S. Degertekin, Design of non-linear steel frames for stress and displacement constraints with semi-rigid connections via genetic optimization, Struct. Multidiscip. Optim. 27 (2004) 259–271.
[74] R. Cucuzza, M. Domaneschi, J. Garcia, M. Rad, M. Habashneh, Construction-based optimization criteria for steel trusses, in: P. Ivanyi, J. Logo, B.H.V. Topping (Eds.), Proceedings of the Sixth International Conference on Soft Computing, Machine Learning and Optimisation in Civil, Structural and Environmental Engineering vol.: CCC 5, Civil-Comp Press, Edinburgh, UK, 2023, https://doi.org/10.4203/ccc.5.1.5. Paper 1.5.
[75] A. Fiore, G. Marano, R. Greco, E. Mastromarino, Structural optimization of hollow-section steel trusses by differential evolution algorithm, Int. J. Steel Struct. 16 (2) (2016) 411–423, https://doi.org/10.1007/s13296-016-6013-1.
[76] S. Gholizadeh, H. Davoudi, F. Fattahi, Design of steel frames by an enhanced moth-flame optimization algorithm, Steel Compos. Struct. 24 (1) (2017) 129–140, https://doi.org/10.12989/scs.2017.24.1.129.
[77] S. Dehghani, A. Vosoughi, M.R. Banan, The effects of rehabilitation objectives on near optimal trade-off relation between minimum weight and maximum drift of 2d steel x-braced frames considering soil-structure interaction using a cluster-based nsga ii, Struct. Multidiscip. Optim. 59 (2019) 1703–1722, https://doi.org/10.1007/s00158-018-2153-6.
[78] O. Hasançebi, S.K. Azad, Discrete sizing of steel frames using adaptive dimensional search algorithm, Period. Polytech. Civ. Eng. 63 (4) (2019) 1062–1079, https://doi.org/10.3311/PPci.14746.
[79] EN1993-1-1, Eurocode 3: Design of Steel Structures - Part 1–1: General Rules and Rules for Buildings, The European Union Per Regulation, Brussels, Belgium, 2005.
[80] M.I. Reitman, W.B. Hall, Optimal structural standardization, Eng. Optim. 16 (2) (1990) 109–128, https://doi.org/10.1080/03052159008941167.
[81] M. Zhu, Topology Optimization of Frame Structures: Design for Constructability and Stochastic Dynamic Loads, Ph.D. thesis, Johns Hopkins University, 2015. accessed: July 10, 2024. URL, https://jscholarship.library.jhu.edu/.
[82] A. Fiore, G. Marano, R. Greco, E. Mastromarino, Structural optimization of hollow-section steel trusses by differential evolution algorithm, Int. J. Steel Struct. 16 (2) (2016) 411–423, https://doi.org/10.1007/s13296-016-6013-1.
[83] R. McNeel, et al., Rhinoceros 3d, version 6.0, Robert McNeel & Associates, Seattle, WA, 2010. Accessed: July 10, 2024. URL, www.rhino3d.com.
[84] R. McNeel, et al., Grasshopper, accessed: July 10, 2024. URL, www.grasshopper3d.com, 2010.
[85] C. Preisinger, Linking structure and parametric geometry, Archit. Des. 83 (2) (2013) 110–113, https://doi.org/10.1002/ad.1564.
[86] N. Tancogne-Dejean, M.J.T. Oliveira, X. Andrade, H. Appel, C.H. Borca, G. Le Breton, F. Buchholz, A. Castro, S. Corni, A.A. Correa, U. De Giovannini, A. Delgado, F.G. Eich, J. Flick, G. Gil, A. Gomez, N. Helbig, H. Hübener, R. Jestädt, J. Jornet-Somoza, A.H. Larsen, I.V. Lebedeva, M. Lüders, M.A. L. Marques, S.T. Ohlmann, S. Pipolo, M. Rampp, C.A. Rozzi, D.A. Strubbe, S. A. Sato, C. Schäfer, I. Theophilou, A. Welden, A. Rubio, Octopus, a computational framework for exploring light-driven phenomena and quantum dynamics in extended and finite systems, J. Chem. Phys. 152 (12) (2020), https://doi.org/10.1063/1.5142502.
[87] E. Zitzler, L. Thiele, Multiobjective evolutionary algorithms: a comparative case study and the strength pareto approach, IEEE Trans. Evol. Comput. 3 (4) (1999) 257–271, https://doi.org/10.1109/4235.797969.
[88] E. Zitzler, Evolutionary Algorithms for Multiobjective Optimization: Methods and Applications vol. 63, Shaker Ithaca, 1999 accessed: July 10, 2024. URL, https://eckartzitzler.ch/.
[89] K.C. Tan, T.H. Lee, E.F. Khor, Evolutionary algorithms for multi-objective optimization: performance assessments and comparisons, Artif. Intell. Rev. 17 (4) (2002) 251–290, https://doi.org/10.1023/A:1015516501242.
[90] E. Zitzler, M. Laumanns, L. Thiele, Spea2: Improving the Strength Pareto Evolutionary Algorithm, TIK Report 103, accessed: July 10, 2024. URL, https://www.research-collection.ethz.ch/, 2001.
[91] D.W. Corne, J.D. Knowles, M.J. Oates, The pareto envelope-based selection algorithm for multiobjective optimization, in: International Conference on Parallel Problem Solving From Nature, 2000, pp. 839–848, https://doi.org/10.1007/3–540–45356-382.
[92] A. Jaszkiewicz, On the performance of multiple-objective genetic local search on the 0/1 knapsack problem-a comparative experiment, IEEE Trans. Evol. Comput. 6 (4) (2002) 402–412, https://doi.org/10.1109/TEVC.2002.802873.
[93] H. Ishibuchi, Y. Nojima, T. Doi, Comparison between single-objective and multi-objective genetic algorithms: performance comparison and performance measures, in: 2006 IEEE International Conference on Evolutionary Computation, 2006, pp. 1143–1150, https://doi.org/10.1109/CEC.2006.1688438.
[94] T. Blickle, L. Thiele, A comparison of selection schemes used in evolutionary algorithms, Evol. Comput. 4 (4) (1996) 361–394, https://doi.org/10.1162/evco.1996.4.4.361.
[95] R. Cucuzza, G. Marano, Structural Optimization Through Cutting Stock Problem, 2024, pp. 210–220, https://doi.org/10.1007/978-3-031-44328-222.
[96] S. Boonstra, K. van der Blom, H. Hofmeyer, M.T. Emmerich, Conceptual structural system layouts via design response grammars and evolutionary algorithms, Autom. Constr. 116 (2020) 103009, https://doi.org/10.1016/j.autcon.2019.103009.
[97] J.D. Delgado, H. Hofmeyer, Automated generation of structural solutions based on spatial designs, Autom. Constr. 35 (2013) 528–541, https://doi.org/10.1016/j.autcon.2013.06.008.
[98] M. Rafiq, M. Rustell, Building information modeling steered by evolutionary computing, J. Comput. Civ. Eng. 28 (4) (2014) 05014003, https://doi.org/10.1061/(ASCE)CP.1943-5487.0000295.
[99] S. Rajeev, C. Krishnamoorthy, Discrete optimization of structures using genetic algorithms, J. Struct. Eng. 118 (5) (1992) 1233–1250, https://doi.org/10.1061/(ASCE)0733-9445(1992)118:5(1233).

[100] M. Kripka, Discrete optimization of trusses by simulated annealing, J. Braz. Soc. Mech. Sci. Eng. 26 (2004) 170–173, https://doi.org/10.1590/S1678-58782004000200008.
[101] C.V. Camp, B.J. Bichon, Design of space trusses using ant colony optimization, J. Struct. Eng. 130 (5) (2004) 741–751, https://doi.org/10.1061/(ASCE)0733-9445(2004)130:5(741).
[102] M. Sonmez, Discrete optimum design of truss structures using artificial bee colony algorithm, Struct. Multidiscip. Optim. 43 (2011) 85–97, https://doi.org/10.1007/s00158-010-0551-5.